AD 745215

AD

USAAMRDL TECHNICAL REPORT 72-18

THE DEVELOPMENT OF A PROBE FOR MEASURING THREE-DIMENSIONAL BOUNDARY LAYERS

By

M. R. Smith

C. B. Cliett

W. W. Livingston

May 1972

D D C

RECEIVED

JUL 17 1972

C

EUSTIS DIRECTORATE

U. S. ARMY AIR MOBILITY RESEARCH AND DEVELOPMENT LABORATORY

FORT EUSTIS, VIRGINIA

CONTRACT DAAJ02-67-C-0016

DEPARTMENT OF AEROPHYSICS AND AEROSPACE ENGINEERING
MISSISSIPPI STATE UNIVERSITY
STATE COLLEGE, MISSISSIPPI

Approved for public release; distribution unlimited.

Reproduced by
NATIONAL TECHNICAL
INFORMATION SERVICE
U S Department of Commerce
Springfield VA 22151

R55

DISCLAIMERS

The findings in this report are not to be construed as an official Department of the Army position unless so designated by other authorized documents.

When Government drawings, specifications, or other data are used for any purpose other than in connection with a definitely related Government procurement operation, the United States Government thereby incurs no responsibility nor any obligation whatsoever; and the fact that the Government may have formulated, furnished, or in any way supplied the said drawings, specifications, or other data is not to be regarded by implication or otherwise as in any manner licensing the holder or any other person or corporation, or conveying any rights or permission, to manufacture, use, or sell any patented invention that may in any way be related thereto.

Trade names cited in this report do not constitute an official endorsement or approval of the use of such commercial hardware or software.

DISPOSITION INSTRUCTIONS

Destroy this report when no longer needed. Do not return it to the originator.

ACCESSION for
CFSTI WHITE SECTION ☑
DDC BUFF SECTION ☐
UNANNOUNCED ☐
JUSTIFICATION .....
.....
BY .....
DISTRIBUTION/AVAILABILITY CODES
DIST. | AVAIL. and/or SPECIAL
A

UNCLASSIFIED
Security Classification

DOCUMENT CONTROL DATA - R & D

(Security classification of title, body of abstract and indexing annotation must be entered when the overall report is classified)

1. ORIGINATING ACTIVITY *(Corporate author)* Mississippi State University Dept. of Aerophysics & Aerospace Engineering State College, Mississippi	2a. REPORT SECURITY CLASSIFICATION Unclassified 2b. GROUP

3. REPORT TITLE

THE DEVELOPMENT OF A PROBE FOR MEASURING THREE-DIMENSIONAL BOUNDARY LAYERS

4. DESCRIPTIVE NOTES *(Type of report and inclusive dates)*

Final Report

5. AUTHOR(S) *(First name, middle initial, last name)*

Michael R. Smith
Charles B. Cliett
William W. Livingston

6. REPORT DATE May 1972	7a. TOTAL NO. OF PAGES 54	7b. NO. OF REFS 5
8a. CONTRACT OR GRANT NO. DAAJ02-67-C-0016 b. PROJECT NO. c. Task 1F162204A14234 d.	9a. ORIGINATOR'S REPORT NUMBER(S) USAAMRDL Technical Report 72-18 9b. OTHER REPORT NO(S) *(Any other numbers that may be assigned this report)* AASE Report No. 72-57	

10. DISTRIBUTION STATEMENT

Approved for public release; distribution unlimited.

11. SUPPLEMENTARY NOTES	12. SPONSORING MILITARY ACTIVITY Eustis Directorate, U. S. Army Air Mobility Research and Development Laboratory, Fort Eustis, Virginia

13. ABSTRACT

A remotely operated boundary layer probe designed for use in three-dimensional boundary layer measurements has been developed. The probe is an adaptation of a Cobra probe. The probe has been used to measure three-dimensional boundary layer flow over a yawed wing. Design procedures and final configurations are described. The experimental investigation indicates that the probe is adequate for measuring steady, three-dimensional boundary layer profiles.

DD FORM 1 NOV 65 1473 REPLACES DD FORM 1473, 1 JAN 64, WHICH IS OBSOLETE FOR ARMY USE.

UNCLASSIFIED
Security Classification

UNCLASSIFIED
Security Classification

14. KEY WORDS	LINK A ROLE	LINK A WT	LINK B ROLE	LINK B WT	LINK C ROLE	LINK C WT
Boundary layer probe						
Three-dimensional boundary layer						

UNCLASSIFIED
Security Classification

DEPARTMENT OF THE ARMY
U. S. ARMY AIR MOBILITY RESEARCH & DEVELOPMENT LABORATORY
EUSTIS DIRECTORATE
FORT EUSTIS, VIRGINIA 23604

This report has been reviewed and is judged to be of interest to agencies engaged in aerodynamic research.

The program was conducted under the technical management of the Aeromechanics Division of this Directorate, including Mr. Clifton G. Wrestler, Mr. John L. Shipley, and Mr. Frederick A. Raitch.

Task 1F162204A14234
Contract DAAJ02-67-C-0016
USAAMRDL Technical Report 72-18
May 1972

THE DEVELOPMENT OF A PROBE FOR MEASURING THREE-DIMENSIONAL BOUNDARY LAYERS

AASE Report No. 72-57

By

M. R. Smith
C. B. Cliett
W. W. Livingston

Prepared by

Raspet Flight Research Laboratory
The Department of Aerophysics and Aerospace Engineering
Mississippi State University
State College, Mississippi

for

EUSTIS DIRECTORATE
U. S. ARMY
AIR MOBILITY RESEARCH AND DEVELOPMENT LABORATORY
FORT EUSTIS, VIRGINIA

Approved for public release;
distribution unlimited.

ii c

TABLE OF CONTENTS

	PAGE
ABSTRACT	iii
LIST OF ILLUSTRATIONS	vi
LIST OF SYMBOLS	viii
1. INTRODUCTION	1
2. DEVELOPMENT OF THE PROBE CONFIGURATION	4
3. CONSTRUCTION OF THE REMOTELY OPERATED BOUNDARY-LAYER PROBE	11
4. PROCEDURES USED TO SECURE EXPERIMENTAL EVIDENCE OF THE PROBE'S RELIABILITY	13
5. COMPARISON OF THEORETICAL AND EXPERIMENTAL RESULTS FOR THREE-DIMENSIONAL BOUNDARY-LAYER FLOW OVER A YAWED WING	16
6. CONCLUSIONS	18
LITERATURE CITED	45
DISTRIBUTION	46

LIST OF ILLUSTRATIONS

Figure		Page
1	General Configuration of the Boundary Layer Problem	19
2	Sketch of Cobra Probe	20
3	Original Pressure Tube Configuration (Configuration A)	20
4	Final Probe Configuration (Configuration E)	21
5a	Yaw Sensitivity - Sensitivity of Total Head to Yaw (All Configurations)	22
5b	Yaw Sensitivity - Sensitivity of Dynamic Pressure to Yaw (All Configurations)	23
5c	Yaw Sensitivity - Sensitivity of Differential Pressure to Yaw (All Configurations)	24
6a	Yaw Sensitivity - Sensitivity of Total Head to Yaw for Probe Configuration E	25
6b	Yaw Sensitivity - Sensitivity of Dynamic Pressure to Yaw for Probe Configuration E	25
6c	Yaw Sensitivity - Sensitivity of Differential Pressure to Yaw for Probe Configuration E	26
7	Exploded View of Manually Operated Boundary Layer Probe	27
8	Schematic of Pressure Tubes and Pressure Transducers	27
9	Oblique View of Initial Probe Unit	28
10	Photograph of Three-Dimensional Probe and Related Instrumentation	29
11	Schematic of Complete Instrumentation Electrical System	30
12	Installation of Boundary Layer Probe in Original Wing Model	31

Figures		Page

13	Yawed Wing Model Mounted in Subsonic Wind Tunnel	32
14a	Boundary-Layer Velocity Profiles Measured on a Yawed Wing, NACA 0012, R = 8.33 x 10^5, Laminar Profile .	33
14b	Boundary-Layer Velocity Profiles Measured on a Yawed Wing, NACA 0012, R = 8.33 x 10^5, Turbulent Profile	34
15	Exploded View of Remotely Operated Boundary Layer Probe	35
16	Photograph of Remotely Operated Boundary Layer Probe . .	36
17	Photograph of Remotely Operated Boundary Layer Probe . .	37
18	Schematic of Wing Model Mounted in Wind Tunnel	38
19	Chordwise Boundary-Layer Velocity Profile, $\Lambda = 30°$, $\alpha = 0°$, $X = 0.20$	39
20	Spanwise Boundary-Layer Velocity Profile, $\Lambda = 30°$, $\alpha = 0°$, $X = 0.20$	40
21	Chordwise Boundary-Layer Velocity Profile, $\Lambda = 45°$, $\alpha = 0°$, $X = 0.20$	41
22	Spanwise Boundary-Layer Velocity Profile, $\Lambda = 45°$, $\alpha = 0°$, $X = 0.20$	42
23	Chordwise Boundary-Layer Velocity Profile, $\Lambda = 60°$, $\alpha = 0°$, $X = 0.20$	43
24	Spanwise Boundary-Layer Velocity Profile, $\Lambda = 60°$, $\alpha = 0°$, $X = 0.20$	44

LIST OF SYMBOLS

c	chord of airfoil
C_p	pressure coefficient $C_p = 1 - (\overline{U}_o/V_R)^2$
H	total pressure
ΔH	differential total pressure
L	reference length
p	dimensional pressure
P'	dimensionless pressure
ΔP	differential pressure
q	dynamic pressure $q = 1/2\rho V^2$
R	Reynolds number $R = LV_R/\nu$
u_L	resultant local boundary-layer velocity
u,v,w	dimensional velocity components in the x, y, and z coordinate directions, respectively
U',V',W'	dimensionless velocity components in x, y, and z coordinate directions, respectively
U_o,V_o	chordwise and spanwise components of boundary-layer potential velocity, respectively
$\overline{U}_o$	magnitude of potential velocity, $U_o = (U_o^2 + V_o^2)^{1/2}$
U_∞	chordwise component of free-stream velocity, $U_\infty = V_R \cos \Lambda$
V_R	magnitude of free-stream velocity
V_∞	spanwise component of free-stream velocity, $V_\infty = V_R \sin \Lambda$
V	a specified velocity
x,y,z	physical coordinates
X',Y',Z'	dimensionless coordinates
α	angle of attack of airfoil

β	angle of yaw of boundary layer probe with respect to local velocity
δ	boundary layer thickness
Λ	angle of yaw of the wing
Ω	vorticity
θ_p	angular position of boundary layer probe with respect to reference line
θ_w	angular position of local velocity vector with respect to reference line
ν	kinematic viscosity
ρ	fluid density

SUBSCRIPTS

at	atmospheric conditions
β	value at a specific angle of yaw
L	local conditions in the flow
o	external to the boundary layer flow
R	reference value or resultant value
ts	wind tunnel test section conditions
∞	free-stream value

1. INTRODUCTION

Measurement of the three-dimensional boundary layer over a body must include the magnitude and the direction of the local flow velocity and the height of the point of measurement above the body surface. In order to accomplish these objectives, it is necessary to consider in greater detail several problems which are of an aerodynamic, structural, and operational nature.

The aerodynamic problems relate primarily to the accuracy of the velocity and direction measurements, the effect of turbulence and velocity gradients upon the pressure measurements, and the effect of the boundary layer probe upon the boundary-layer flow itself. The physical dimensions of the boundary layer require that the instrumentation be very small so as not to unduly disburb the local flow and that the direction of the local flow be measured very accurately. Due to the significant velocity gradient that exists between the surface and the external flow, it is necessary that the instrumentation be capable of measuring both large and small velocities very accurately. In addition, it is necessary to consider the effect of turbulence and velocity gradients upon velocity measurements.

MacMillan (Reference 1) has investigated the effect of viscosity on pressure measurements at low Reynolds numbers. Measurements were made of pressure in a flattened, blunt nose, Pitot tube in an airstream at Reynolds numbers ranging from 10 to 1000 (R based on the external height of the tube). Three tubes were used having cross sections with ratios of width to height (W/H) of 7 to 11. The results were expressed in terms of a pressure coefficient, $C_p = (P-p)/1/2\rho V_R^2$, where P is the pressure in the Pitot tube and p and V_R are the static pressure and velocity in the undisturbed airstream. It was found that Cp decreased below one for all the tubes, although earlier measurements had shown that this did not occur with circular tubes. The maximum decrease was about one percent at a Reynolds number of 60. When the values of C_p for the height ratios (W/H) of 7 and 11 were plotted against Reynolds number based on internal height of the tube orifice, the curves were in a good agreement. There was a general trend toward this limiting curve as the ratio (W/H) ranged from the value of 1 (a circular Pitot tube) to a value of 11. A width-to-height ratio of 7 was used for the probe that was employed in the present investigation.

An investigation by Bradshaw and Goodman (Reference 2) on the effect of turbulence on static pressure measurement errors indicated that the error in static tube reading, due to the turbulent fluctuations, depends on the ratio of the size of the tube to the size of the typical turbulent eddies. The pressure reading of tubes of the size likely to be used in practice is nearer to the actual static pressure than to either of the theoretical predictions for tubes which are very small, or very large, compared with the turbulent eddies. In the range of sizes likely

to be used in turbulent flow, static pressure tubes of the size ranging from 0.047 to 0.0157 inch outside diameter indicated closer to the true static pressure on the center line of a circular jet than to either of the theoretical values for very large or very small tubes. The effect of Reynolds number is very small, at least for Reynolds numbers greater than one. It is suggested that the best procedure is to omit any correction for shear flow turbulence unless a proper investigation can be made in the flow actually being used. An investigation by Ower and Pankhurst (Reference 3) on total pressure measurements showed that the effect of turbulence of the intensity encountered in the wind tunnel test program produced a negligible error in the total pressure measurements.

An investigation by MacMillan (Reference 4) on the effect of shear flow on Pitot-tube pressure measurements indicated that when a Pitot tube is used in a pipe or boundary layer, the shear at the wall may cause the pressure in the Pitot tube to differ from the true total pressure on the axis of the tube. To investigate these effects, measurements were made in a circular pipe with turbulent flow using Pitot tubes of different external diameter. Some supporting experiments were made in a turbulent boundary layer on a flat plate with a zero pressure gradient. It was found that the effect of shear alone could be conveniently expressed as a displacement of the "effective center" of the tube toward the region of higher velocity. The value of the displacement was found to be independent of the Reynolds number of the velocity gradient. When the tube is near a wall, an additional correction must be applied. If this additional correction is expressed as a correction, u, to the measured velocity, U, it was found that u/U was independent of Reynolds number within the accuracy of the experiments. In the present investigation it was found that for flattened tubes, with width-to-height ratios of 7 to 11, the displacement of the effective center of the tube was negligible; however, some error was introduced in the pressure reading when the tube was very near the wall. This error resulted in an increase in the computed velocity which is opposite to the "wall effect" for circular tubes. Development of a method of correcting for this error was unsuccessful; therefore, it was necessary to visually delete the first 1 to 3 velocity points on the wall side of the boundary layer. In the case of laminar flow, this posed no problem, since the slope of the velocity profile was well defined prior to reaching the erroneous points. However, for turbulent profiles, it was sometimes difficult to determine which points should be deleted.

In order to determine the effect of the yaw of a wing upon the development of the three-dimensional boundary layer probe, it was necessary to consider the geometry of the flow problem and the magnitude of the pressure and velocity involved. The coordinate system used to define the flow over the yawed wing is shown in Figure 1. Since the dynamic pressure of the test section (q_{ts}) is measured, the free-stream

velocity (V_R) may be calculated from the following equation:

$$V_R = (2q_{ts}/P_{ts})^{1/2} \tag{1}$$

Then the chordwise and spanwise components of the free-stream velocity are given by the following equations:

$$U_\infty = V_R \text{ Cos } \Lambda$$

$$V_\infty = V_R \text{ Sin } \Lambda \tag{2}$$

If the pressure coefficient at a particular chord station is known from either experimental or theoretical results, the potential velocity at a particular station may be found from the definition of the pressure coefficient

$$\overline{U}_o = V_R(1-C_p)^{1/2} \tag{3}$$

and the chordwise and spanwise components of the potential flow are given by the following equations:

$$U_o = \overline{U}_o \text{ Cos } \Lambda$$

$$V_o = \overline{U}_o \text{ Sin } \Lambda \tag{4}$$

The local dynamic pressure (q_L) at a point in the boundary layer can be found from the probe measurements as will be shown. With this known quantity, the local velocity in the boundary layer (u_L) is given by the following formula:

$$u_L = (2q_L/P_{ts})^{1/2} \tag{5}$$

and its chordwise and spanwise components are given by the following equations:

$$u = u_L \text{ Cos } \theta_w$$

$$v = u_L \text{ Sin } \theta_w \tag{6}$$

where θ_w is the angle between the local resultant velocity (u_L) and the chord of the wing, as shown in Figure 1. Using the preceding equations, the nondimensional velocities may be calculated and used to determine the boundary-layer characteristic parameters.

2. DEVELOPMENT OF THE PROBE CONFIGURATION

Review of previous research on the development of instrumentation to measure boundary-layer velocities and local flow direction indicated that the Cobra probe (Figure 2) was probably best suited for adaptation as a three-dimensional boundary layer probe. The Cobra probe is a specialized probe which has been used previously to measure both the total head and the flow direction of potential flows. The Cobra probe is composed of three individual tubes--the center tube measures the total pressure in the flow and the two lateral tubes measure the flow direction. The sensitivity of the probe to the direction of flow can be adjusted by varying the angle at which the yaw probes are cut off. The direction of the flow is then determined by adjusting the angular position of the probe until the pressure differential between the two yaw probes is zero.

In making boundary layer measurements, it is desirable to make the measurements at a particular chordwise station to facilitate comparison of the results. However, with the use of a probe, such as the Cobra probe, in which the pressure tubes do not pivot about the given chordwise station, the chordwise station will vary with the yaw of the wing, thus making it difficult to compare boundary layer profiles at a particular chordwise station. In order to minimize this effect, it was desired to make the length of the probe head as small as possible without introducing appreciable error in the total pressure and yaw measurements due to the proximity of the vertical shaft of the probe.

The dimensions of the 3-tube configuration were established by tests to determine the sensitivity of the probe to the probe yaw angle (β). It was desired to make the center tube as short as possible with a low sensitivity to changes in the yaw angle. The original dimensions of the probe are shown in Figure 3. Tests were made with successively shorter total head tubes until a satisfactory configuration (Configuration E) was obtained as shown in Figure 4. The sensitivity data are presented as graphs of the dimensionless total pressure, dynamic pressure, and pressure differential versus the probe yaw angle (β). The quantities were nondimensionalized with respect to the free-stream values and defined as follows:

$$C_1' = \frac{H_\beta}{H_\infty}, \quad C_1 = \frac{q_\beta}{q_\infty}, \quad C_2 = \frac{\Delta P}{q_\infty} \tag{7}$$

It was found that the best results could be obtained by flattening the pressure tubes to a thickness of 0.010 inch. The sensitivity data for the final configuration are shown in Figures 5A, 5B, 5C, 6A, 6B, and 6C.

CONSTRUCTION OF MANUALLY OPERATED PROBE

Since the angle of yaw between the probe and the local flow could be obtained from the pressure measurements, it was necessary to measure the angular position of the probe with respect to some reference in order to determine the direction of the local flow with respect to the reference. In order to measure the angular position of the probe (θ_p), a variable resistance potentiometer was built into the probe housing. This was accomplished by attaching a resistance wafer from a potentiometer to the bottom of the movable cylinder. A metal pointer, grounded on the probe housing, made contact with the wafer and a voltage potential was impressed across the circuit, causing a current flow through the wafer. As the probe was rotated into the flow, the cylinder and wafer rotated also, thus changing the distance that the current had to flow through the wafer, or in other words, changing the resistance of the complete circuit. A calibration curve of angular position from the chord lines versus resistance was generated to determine the position of the probe during the boundary layer measurements.

The vertical traverse of the boundary layer probe was accomplished by a simple jackscrew arrangement, which is shown in the section view of the movable cylinder in Figure 7. The screw was adjusted manually to raise and lower the probe.

PRESSURE INSTRUMENTATION AND CALIBRATION

The operating principle of the three-dimensional boundary layer probe is based upon Bernoulli's equation, which states that the total pressure of a fluid flow is equal to the sum of the static pressure and the dynamic pressure. Written in terms of the boundary-layer quantities, Bernoulli's equation becomes

$$H_L = P_L + 1/2\rho_{ts}u_L^2 \tag{8}$$

Thus, if H_L and P_L are measured, the local velocity in the boundary layer may be found from the following equation:

$$u_L = [(2/\rho_{ts})(H_L - P_L)]^{1/2} \tag{9}$$

Ideally, it would be desirable to measure both H_L and P_L at the same time and with the same instrument; however, size limitations of the probe made this approach impractical. Therefore, the local static pressure distribution on the yawed wing was measured prior to making the boundary layer measurements, and the nondimensional pressure coefficients (C_p) were tabulated for future reference. By making the boundary layer measurements at the same free-stream Reynolds number, the pressure coefficients could be used for calculation of the boundary layer velocity without introducing possible Reynolds number effects into the

pressure measurements. This procedure is consistent with the assumption in boundary layer theory that the static pressure in the boundary-layer coordinate direction is constant through the boundary layer. With the static pressure available from the previous pressure measurements, the requirements on the probe reduced to the following: (1) to measure the total pressure at each point in the boundary layer, (2) to measure the direction of the flow with respect to some arbitrary reference, and (3) to vertically traverse the boundary layer.

Upon establishment of the final configuration of the boundary-layer probe, it was possible to proceed with developing instrumentation to record the required pressure and position measurements and establish the configuration of the probe housing. The pressure measurements were made through the use of two differential pressure transducers, as shown in Figure 8. The No. 1 pressure transducer was used to measure the total pressure in the boundary layer flow, with respect to a given reference pressure, which in this case was taken as the atmospheric pressure. The No. 2 pressure transducer was used to measure the differential pressure between the yaw tubes, denoted as left and right yaw tubes. The differential pressure across the front of the probe could be correlated with the probe yaw angle (β); and thus, when $\Delta P = 0$, the probe was pointed directly into the flow and the center probe was reading the total pressure. This probe configuration was mounted in a movable cylinder, which was in turn mounted in a metal housing containing the two pressure transducers. The housing could then be mounted inside the airfoil, and by drilling a small hole in the airfoil surface, the boundary layer probe could be passed through the surface and into the boundary layer. The dimensions of the initial housing were 2-1/4 inches by 1 inch by 1 inch. A photograph of the complete initial unit is shown in Figure 9.

The transducers for the total pressure and differential pressure were Statham 0 to 5 psi differential pressure transducers. Pressure transducer No. 1 was used to measure the total pressure and was referenced to the atmospheric pressure, as shown in Figure 8. The output of the transducer was a voltage reading (ΔH_1) which was converted into pressure in pounds per square foot (ΔH_2). The equation used to calculate the local velocity in the boundary layer was developed as follows:

$$H_{at} = P_{at} + \cancel{q_{at}}^{0} \tag{10}$$

$$H_L = P_L + q_L \tag{11}$$

Subtracting equation (10) from equation (11),

$$\Delta H_L = H_L - H_{at} \tag{12}$$

$$= P_L + q_L - P_{at}$$

or $$q_L = \Delta H_L - P_L + P_{at} \tag{13}$$

and $$u_L = (2q_L/\rho_{ts})^{1/2} \tag{14}$$

Since the pressure transducers were of the strain-gage type, with a deflectable diaphragm, there was a possibility that the diaphragm would not deflect symmetrically, and it was necessary to calibrate the transducer both for the condition $H_L > P_{at}$ and for $H_L < P_{at}$. These calibration curves were generated by imposing a pressure differential across the transducer with a Betz manometer. The electrical circuit was set up so that a positive millivolt reading corresponded to the condition $H_L > P_{at}$ and a negative reading corresponded to the condition $H_L < P_{at}$.

The No. 2 yaw transducer was used to measure the pressure differential between the yaw tubes, which were labeled P_r and P_l, so that observers looking into the flow would see P_r on the right side and P_l on the left side (Figure 8). The yaw transducers were also calibrated for both right and left deflections of the diaphragm corresponding to $P_l > P_r$ and $P_l < P_r$, respectively. The electrical circuit was set up so that the sign convention would be applied corresponding to the sign of the voltage readout. The calibration curve generated by this scheme, ΔP_l versus ΔP_2, had to be related to the probe yaw angle (β). This was done by using the previously acquired C_2 versus β curve which was generated during the probe configuration test. Using this information, a curve of ΔP_2 versus β was obtained. That is, for a particular value of β, a corresponding value of C_2 could be calculated by $\Delta P_2 = C_2 q_L$. During the preliminary boundary layer measurements, it was found that the ΔP_l measured by the probe was dependent on Reynolds number; therefore, this procedure of finding the yaw angle was abandoned. Instead, it was decided to zero the ΔP reading at each data collection point; then, correction for yaw angle would not be necessary. In an automated version of the probe, this would present no difficulty; however, in the manually operated probe, it required that several trials be made in order to exactly zero the reading.

The probe angular position potentiometer was calibrated prior to mounting the instrument in the airfoil by a simple procedure, whereby the scribed center line of the probe was aligned to a protractor in a position that would correspond to its alignment with the chord of the airfoil. Then, as the probe was moved to angles away from this reference, the resistance in ohms was read directly on a digital voltmeter. With this information, a graph of probe position angle (θ_p) versus resistance was made.

The vertical position of the probe was determined by counting the number of turns of the vertical traverse screw. There were 80 threads per inch on the traverse screw, which corresponded to 0.0125 inch of traverse per revolution. A dial indicator gage was used to check the traverse of the screw per revolution, and the results indicated that 0.0125 inch per revolution was correct. Approximately one-eighth of a turn of slack was encountered in the system; however, the boundary-layer traverse was always

made in one direction. Therefore, this did not pose a problem in the experimental program.

In order to insure that a constant dynamic pressure was maintained in the tunnel test section, a Pitot-static tube was mounted in the test section and connected to a third pressure transducer. This system was calibrated using a Betz manometer in the same manner as described previously.

The power supply for the instrumentation system was a Hewlett-Packard Model 6251A, ±15-volt unit. Balance boxes were used in conjunction with transducers No. 1 and No. 2 to insure that an excitation voltage of five volts was supplied to the transducers, and to aid in proper zeroing of the transducer output. The output of transducers No. 1 and No. 2 was amplified using a Kintel, Model 114A, differential amplifier. The output of transducer No. 3 was stabilized and amplified with a specially constructed oscillator-amplifier. The output of transducers Nos. 1, 2, and 3 and the output of the resistance wafer were all connected to a rotary switch located on the front of the amplifier rack. The transducer output voltages and the resistance of the probe position wafer were then read at this common point with a Honeywell Digitest digital voltmeter. Figure 10 shows the major components of the system, and a schematic of the electrical circuit is shown in Figure 11.

INSTALLATION OF THE BOUNDARY-LAYER PROBE IN THE WING MODEL

The wing model used for the preliminary tests of the boundary-layer probe possessed an NACA 0012 airfoil section and a 12-inch chord. The model was constructed with wooden spars and ribs and was covered with a fiber-glass skin. A removable panel on the lower surface of the airfoil afforded access so that the probe could be attached internally to the upper surface of the wing. Figure 12 shows the lower surface of the airfoil with the panel removed and the probe mounted. At each chord station, the extreme front of the pressure tube was placed over the point where the static pressure had been measured previously. The top of the movable cylinder and the heads of the four attachment screws were mounted flush with the airfoil surface; and, during the test runs, these areas were sealed with modeling clay which could be contoured to the surface contour.

The airfoil was thick enough to accommodate the probe housing between the 20-percent and 60-percent chord position. In order that the airfoil surface in front of the probe would always be smooth, the probe was installed at the 60-percent chord position for the first test. The boundary layer measurements were then made at angles of attack of 0, 4, 8 and 12 degrees. Subsequent tests at these same angles of attack were made with the probe positioned at 50-, 40-, and 20-percent chord, respectively. Figure 13 shows the wing model mounted in the tunnel at a yaw angle of 30 degrees.

In order to determine the region of influence of the boundary-layer probe on the boundary-layer flow, a sublimation technique of flow visualization was employed. This flow visualization method consisted of spraying a saturated solution of naphthalene and petroleum ether on the airfoil surface. The solution formed a white coat which contrasted well with the black wing surface. Photographs of the surface under test conditions were taken, and the naphthalene crystals were quickly eroded in regions of high surface shear. From these tests, it was possible to substantiate that the boundary-layer probe caused a very small separated region in the boundary-layer flow and that this perturbation was not amplified, except at angles of attack near the stall angle.

These tests and all of the subsequently mentioned wind tunnel measurements were conducted in the closed-circuit, subsonic wind tunnel at Mississippi State University. The test section of this tunnel is octagonal with maximum dimensions of 3 feet by 4 feet by 5 feet long. The usable speed range is from 30 feet per second to 180 feet per second.

PRELIMINARY MEASUREMENTS ON THE YAWED WING

For each test run, the boundary-layer probe was mounted at a particular chord station with the airfoil at a specific angle of attack. The initial height of the probe above the surface was determined with a mechanical feeler gage, and the subsequent heights were determined by counting the turns of the traversing screw. Before starting the tunnel, the probe was aligned with the estimated flow direction.

The wind tunnel was operated at the same dynamic pressure which had been used in measuring the pressure coefficients. This dynamic pressure was maintained in the test section by referring to the output of the Pitot-static transducer. When the reference dynamic pressure was achieved, the differential pressure across the yaw probe was checked to see if the probe was pointed directly into the local flow. If ΔP was equal to zero, the data were recorded; but if $\Delta P \neq 0$, the tunnel was stopped and the probe was rotated toward the zero yaw position, using the previously mentioned zeroing scheme. It was found that the high sensitivity of the ΔP reading to even small rotations made it very difficult to zero the reading, but care was taken to make $\Delta P = 0$ at each data point. Readings were then taken of ΔH_1, θ_p, tunnel air temperature, and tunnel dynamic pressure. Atmospheric pressure was read with a standard mercury barometer, and temperature in the test section was obtained from a bimetal, strip-type thermometer which was mounted in the test section.

Having obtained the necessary data for a particular height (z) above the surface of the airfoil, the probe was then raised to a new height and the process was repeated. This was done until the ΔH_1 reading was the same

for two or more consecutive heights. When this occurred, it was assumed that the probe was out of the boundary layer and the run was terminated. The airfoil was then moved to a new angle of attack, and the whole process was repeated.

The process was very tedious and time-consuming, which increased the possibility of human error. The minimum time required to measure one profile was approximately two hours. It became obvious that while a thorough study of three-dimensional boundary layers on a yawed wing could utilize this basic instrumentation, it would be necessary to have the process automated in order to increase the rapiditiy and accuracy of the measurements. Typical examples of the experimentally measured boundary-layer profiles are shown in Figures 14a and 14b.

3. CONSTRUCTION OF THE REMOTELY OPERATED BOUNDARY-LAYER PROBE

Having determined that the boundary-layer probe configuration was suitable for measuring three-dimensional boundary layers, it was decided to redesign the probe so that it could be remotely operated to extend its overall capabilities. The most time-consuming factor involved with the manually operated probe was that of getting the probe aligned with the local flow direction; therefore, the predominant consideration in the redesign was that of aligning the probe into the local flow. In addition, consideration was also given to the possibility of mechanizing the traversing mechanism, and also modifying the probe, so that boundary layers of greater thickness could be measured.

After considerable redesign, a new system was developed whereby the probe could be rotated and traversed remotely. In addition, the traversing distance was approximately tripled to a maximum of 0.625 inch, while the total depth of the probe was reduced from 1 inch to 0.75 inch. An exploded view of the instrumentation is shown in Figure 15, and a detailed photograph is given in Figure 16.

The remotely operated probe is composed of two concentric cylinders which are driven by worm gear drives that are remotely operated through a flexible shaft system. The boundary layer probe (G) was designed so that it could traverse through the cylinder (F); however, the probe was fixed so that it could not rotate within the cylinder (F). Gear (E) was rigidly attached to the cylinder (F) and driven by worm gear (A) in order to rotate the probe into the local flow direction. A threaded collar was attached to the end of the boundary-layer probe (G), and the collar extended into the cylinder (C), which was threaded internally. Cylinder (C) was mounted internally to the cylinder (F) and rigidly locked so that it could not move axially. Cylinder (C) was rotated by the worm gear (B) in order to traverse the boundary-layer probe through the boundary-layer flow. Each revolution of gear (B) corresponded to a 0.001-inch traverse of the boundary layer probe. Obviously, some error was introduced into the height measurement due to the rotation of cylinder (F) with respect to cylinder (C); however, the boundary-layer probe was aligned in the direction of the local potential flow at the beginning of each test such that the error introduced by rotation of cylinder (F) was less than one-thousandth of an inch for all cases and was thus neglected in the final position calculations. A photograph of the complete boundary-layer probe instrumentation and the mechanism to remotely control the probe is shown in Figure 17. The digital counter attached to the driving mechanism was calibrated to read the vertical position of the probe in thousandths of an inch. During the boundary-layer measurements, the probe was started with the lower surface of the probe 0.0015 inch above the wing surface, which positioned the center of the probe at vertical station 0.0065 inch. By starting the digital counter at this reading, it was possible to read

the height of the probe above the surface directly from the counter. The boundary-layer instrumentation was installed in the wing model in a manner similar to that explained previously, and the related pressures were recorded in an identical manner. The boundary-layer velocity measurements were initiated at the wall side of the boundary layer and progressively sampled in the direction of the external flow. The initial position of the center line of the probe was at 0.0065 inch above the wing surface. At this height, the angular position of the probe was adjusted until the probe was pointing in the direction of the local flow, and then pressures and related data were recorded manually. The probe was then raised to the next position above the surface, and the process was repeated until the pressure readings indicated that the probe was outside the boundary layer. With one person operating the remote controls and another reading the instrumentation signals, it was possible to obtain a complete boundary-layer velocity profile in 10 to 15 minutes as opposed to 2 to 3 hours with the manually operated probe.

4. PROCEDURES USED TO SECURE EXPERIMENTAL EVIDENCE OF THE PROBE'S RELIABILITY

In order to confirm the feasibility of the probe for practical three-dimensional boundary-layer measurements, an extensive wind tunnel test program was conducted. A 12-inch-chord, 66-inch-long wing model with an NACA 0012 airfoil section was used in this program. Selection of this particular airfoil section was made because this section is frequently used as the airfoil in helicopter rotors and it was anticipated that subsequently the probe would be utilized to measure boundary-layer flow on a helicopter rotor blade in the hover mode.

Extreme care was used in the construction of the model to insure that the leading edge was formed to the proper contour of the NACA 0012 airfoil. The leading edge was carefully milled and checked systematically using a template of the airfoil. Waviness of the airfoil aft of the leading edge was checked to assure that waviness was less than 0.001 inch per inch over the test area.

Static pressure taps were flush-mounted at three spanwise stations to measure the pressure distributions around the airfoil and to determine the spanwise variation in the pressure. Thirty-one static taps were located at each spanwise station, and these were distributed with 15 taps on the top side, 15 taps on the bottom side, and 1 tap at the leading edge (Figure 18).

INSTALLATION OF THE WING MODEL IN THE WIND TUNNEL

The wing model was mounted vertically in the wind tunnel, with the lower end of the airfoil resting on the tunnel floor and the upper end extending through the tunnel roof (Figure 18). The cylindrical spar extended approximately 16 inches past the end of the airfoil and was mounted in a universal-joint type mount, which permitted the airfoil to be yawed or pitched independently. The lower mount was attached to the tunnel in one position, and the yaw angle of the airfoil model was changed by moving the upper mount along a circular path, as shown in Figure 19. The wing model was mounted successively at yaw angles of 0, 30, 45, and 60 degrees, and the mounting brackets were attached to assure that the model was mounted at the same angle of yaw during all subsequent tests; in addition, the yaw angle was measured prior to each test to verify this.

MEASUREMENT OF AIRFOIL PRESSURE DISTRIBUTIONS

Due to a slight rotation in the wind tunnel flow, it appeared impractical to try to adjust the zero angle of attack of the airfoil at

each angle of yaw by a geometric zeroing process. In order to determine the zero angle of attack of the airfoil at the station where the boundary-layer measurements were being made, the pressure distribution around the leading edge of the airfoil was measured and the wing model was adjusted until the pressure distributions on each side were identical. Upon locating the zero angle of attack at a particular angle of yaw, the trailing-edge position was marked to facilitate returning to the same zero angle of attack. However, in each case when the airfoil was mounted at a new angle of yaw, the pressure distributions were measured to determine when the airfoil was set at its zero angle of attack.

The airfoil pressure distributions were measured at each angle of yaw prior to boring any holes in the wing model to mount the boundary-layer probe. The pressure distributions were reduced to a nondimensional pressure coefficient form using the resultant wind tunnel velocity as the reference; thus, $C_P = 1 - (\bar{U}_0/V_R)^2$.

INSTALLATION AND CALIBRATION OF BOUNDARY-LAYER PROBE

The boundary-layer-probe housing was mounted internal to the airfoil and attached to the upper surface of the wing using four flush-mounted screws. A hole approximately twice the diameter of the probe shaft was bored in the wing surface to permit insertion of the probe through the surface and to permit angular movement of the probe during the traverse of the boundary layer. The electrical wires and pressure tubes were routed along the circular spar and out the bottom of the tunnel to the control panel. The holes surrounding the boundary-layer probe and the regions over the flush-mounted screws were sealed to assure that the surface was smooth and that air leaks would not occur which could cause boundary-layer separation.

Two flexible shafts were employed to change the boundary-layer-probe position. One shaft was employed to change the angular position of the probe by driving the worm gear (Gear A) on the side of the transducer housing (Figure 17), and the second shaft was employed to operate the worm gear (Gear B) which drives the traversing mechanism. The shaft which changed the angular position was routed to the control panel, and a graduated dial was employed to determine the approximate position of the boundary-layer probe. Due to approximately one-eighth of a revolution of slack in the cable, the indicator gave only a rough estimate of the position of the probe; however, the resistance wafer attached to the bottom of the probe gave a very accurate measurement of the angular position. The shaft which controlled the vertical height of the probe above the surface was likewise routed to the control panel and attached to a geared mechanism which had a three-to-one gear reduction between the shaft and the driving gear. The driven shaft was attached to one side of the driven gear and a Veeder-Roots counter was attached to the other side of the gear. The gearing on

the drive mechanism was designed such that one unit on the Veeder-Roots counter corresponded to a vertical movement of 0.001 inch on the probe.

MEASUREMENT OF BOUNDARY-LAYER VELOCITY PROFILES

The boundary-layer velocity profile measurements were made following the measurement of the pressure distributions around the airfoil. The profile measurements were started by mounting the boundary-layer probe at the 60-percent chord position and taking all measurements for the first angle of yaw. The airfoil was then mounted at the next angle of yaw, and the boundary-layer measurements were repeated. This procedure was continued until all the desired angles of yaw had been completed with the boundary-layer probe mounted at the 60-percent position. The probe was then mounted at 50-percent chord in the preceding manner. Employing the foregoing procedure, boundary-layer measurements were made at chordwise positions of 20, 30, 40, and 50 percent and at angles of yaw of 0, 30, 45, and 60 degrees.

5. COMPARISON OF THEORETICAL AND EXPERIMENTAL RESULTS FOR THREE-DIMENSIONAL BOUNDARY-LAYER FLOW OVER A YAWED WING

The classical boundary layer equations for laminar flow on an infinite, yawed wing are derived based on the assumption that the inviscid flow is irrotational ($\Omega_z = 0$). The irrotationality of the inviscid flow and the assumed spanwise invariance of the inviscid flow require that the spanwise component of the inviscid flow must be constant. These classical boundary-layer equations are listed below:

$$u \frac{\partial u}{\partial x} + w \frac{\partial u}{\partial z} = U_0 \frac{\partial U_0}{\partial x} + \nu \frac{\partial^2 u}{\partial z^2}$$

$$u \frac{\partial v}{\partial x} + w \frac{\partial v}{\partial z} = \nu \frac{\partial^2 v}{\partial z^2}$$

$$\frac{\partial u}{\partial x} + \frac{\partial w}{\partial z} = 0 \tag{15}$$

The boundary conditions for these equations are:

$$z = 0: \quad u = v = w = 0$$

$$z = \infty: \quad u = U_0(x,y), \; v = \text{constant} = V_\infty$$

Smith (Reference 5) has recently produced experimental evidence for a yawed infinite wing which shows that variations in the spanwise components of the external flow on the order of ±30 percent of V_∞ occur. This evidence indicates that the classical boundary layer equations for an infinite, yawed wing where the assumption is made that the inviscid flow is irrotational ($\Omega_z = 0$) cannot be accurately used to approximate a three-dimensional laminar boundary layer. Smith presents a theoretical analysis which is based on the assumption that the flow outside of the boundary layer is rotational and inviscid. The resulting boundary-layer equations are:

$$u \frac{\partial u}{\partial x} + w \frac{\partial u}{\partial z} = - \frac{1}{\rho} \frac{\partial p}{\partial x} + \nu \frac{\partial^2 u}{\partial z^2}$$

$$u \frac{\partial v}{\partial x} + w \frac{\partial v}{\partial z} = - \frac{1}{\rho} \frac{\partial p}{\partial y} + \nu \frac{\partial^2 v}{\partial z^2}$$

$$\frac{\partial u}{\partial x} + \frac{\partial w}{\partial z} = 0 \tag{16}$$

The associated boundary conditions for these equations are:

$$z = 0: \quad u = v = 0$$

$$z = \infty: \quad u = U_0, \; v = V_0$$

Smith (Reference 5) presents a numerical solution using finite-difference techniques for the classical boundary-layer equations and for the more general analysis considering the flow outside of the boundary layer to be rotational and inviscid. Defense of this analysis is presented is his paper. Only the results for specific cases will be presented as a part of this paper, and these results are intended only for comparison purposes to illustrate the use and reliability of the remotely operated boundary-layer probe.

Experimental data are plotted on each graph for comparison purposes with the numerical results for both the classical yawed wing case (V_0 = constant = V_∞) and for the case of the yawed wing with rotational and inviscid flow ($V_0 = V_0(x)$). In each case, there is only one plot for the chordwise velocity profile V/V_0. The inviscid chordwise velocity distribution was the same in each case,and the numerical solutions produced identical results.

Figures 19 through 24 present the comparison of the numerical solutions and the experimental data. The boundary-layer velocity profiles presented are for the 20-percent chord station, for sweep angles of 30, 45, and 60 degrees. The experimental evidence in each case follows the trend of the predicted data and is, in fact, in reasonable agreement in each case. Smith (Reference 5) compares experimentally measured boundary-layer velocity profiles with the same theory for a number of other chord stations, and the comparisons remain good.

6. CONCLUSIONS

The boundary-layer probe described in this report is adequate for measuring steady, three-dimensional boundary-layer profiles. Further investigations on the probe need to be conducted to establish a wall correction factor for the probe and to determine the effect of local Reynolds number on the accuracy of the pressure measurements.

Additional consideration needs to be given to the possibility of measuring both the total and static pressures with the boundary-layer probe. Presently the static pressure must be measured independently of the total pressure in the boundary layer.

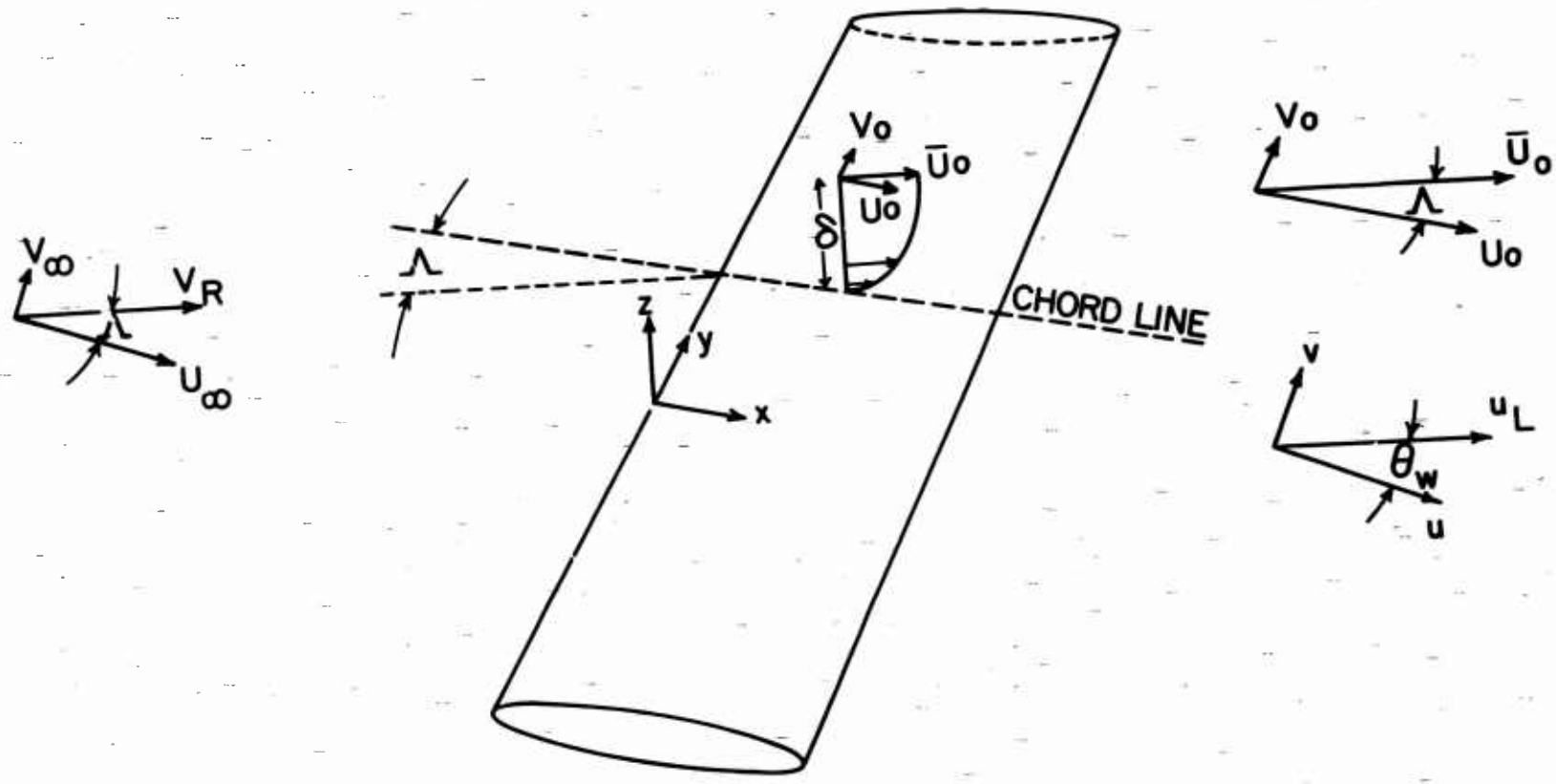

Figure 1. General Configuration of the Boundary Layer Problem.

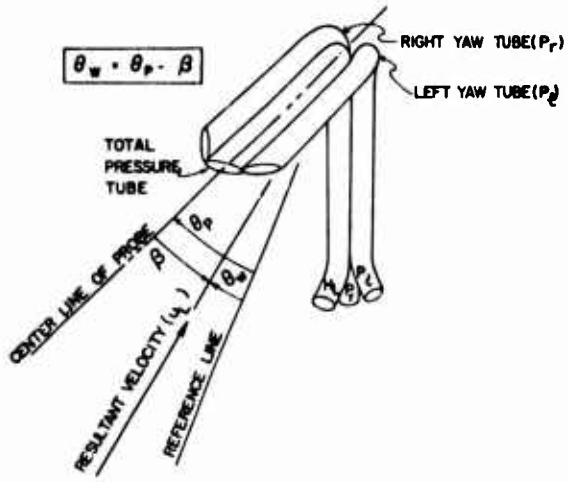

Figure 2. Sketch of Cobra Probe.

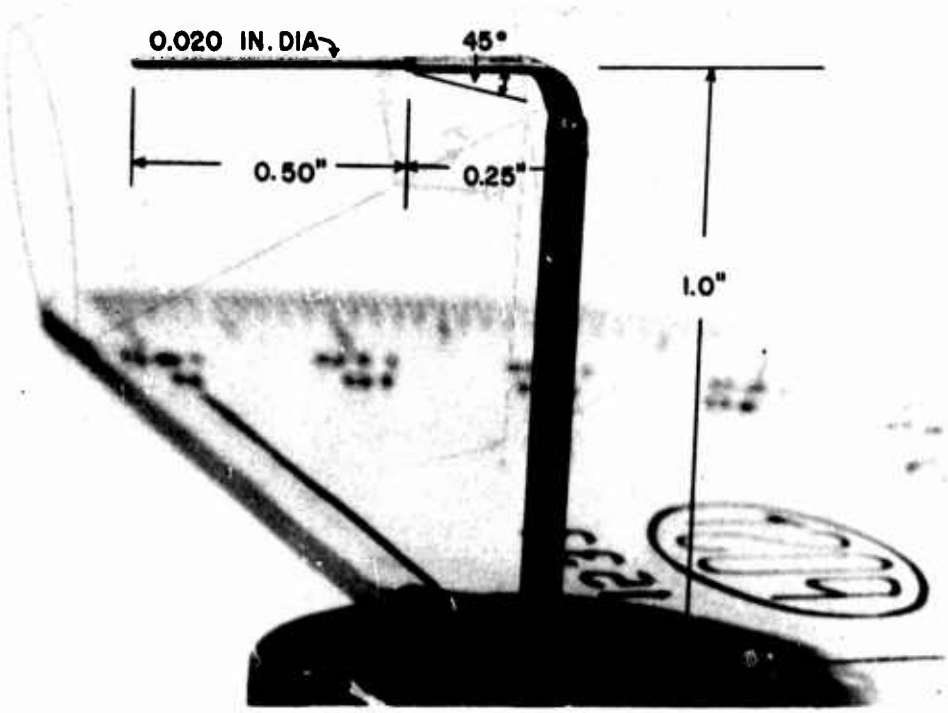

Figure 3. Original Pressure Tube Configuration (Configuration A).

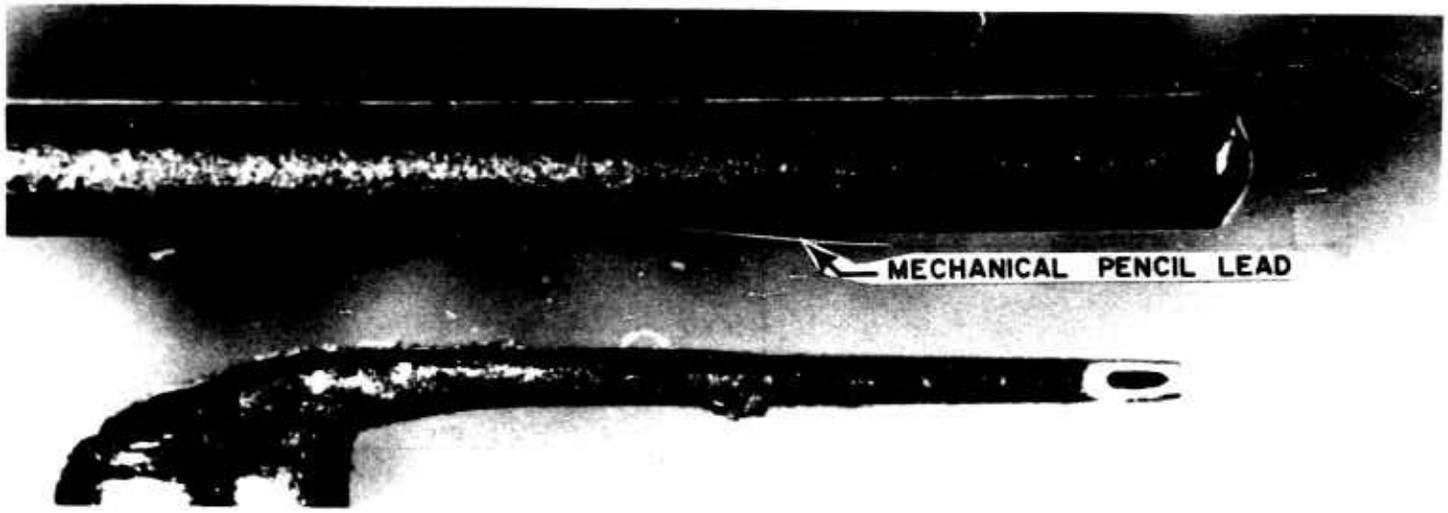

a. Side View.

b. Front View.

Figure 4. Final Probe Configuration (Configuration E).

Reproduced from best available copy.

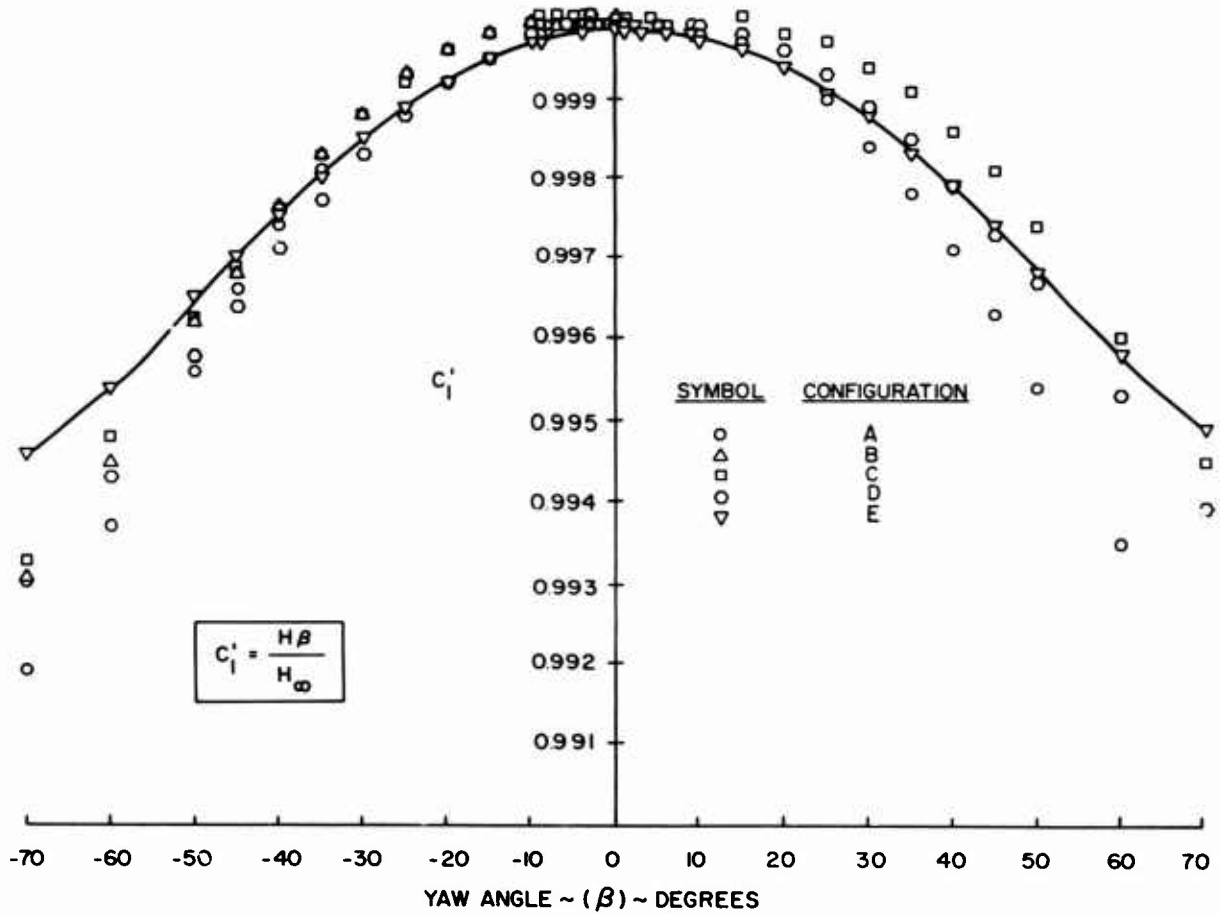

Figure 5a. Yaw Sensitivity - Sensitivity of Total Head to Yaw (All Configurations).

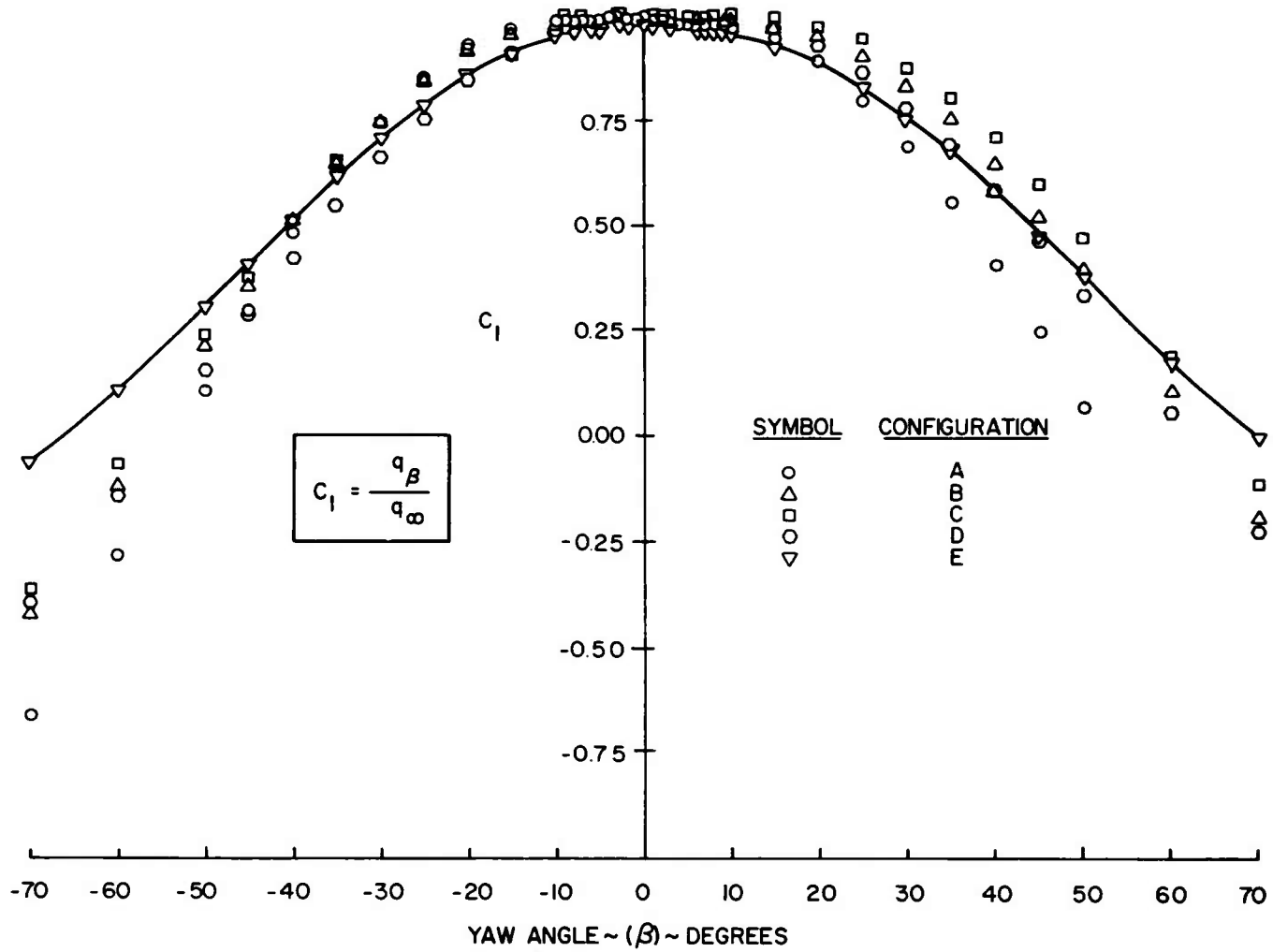

Figure 5b. Yaw Sensitivity - Sensitivity of Dynamic Pressure to Yaw (All Configurations).

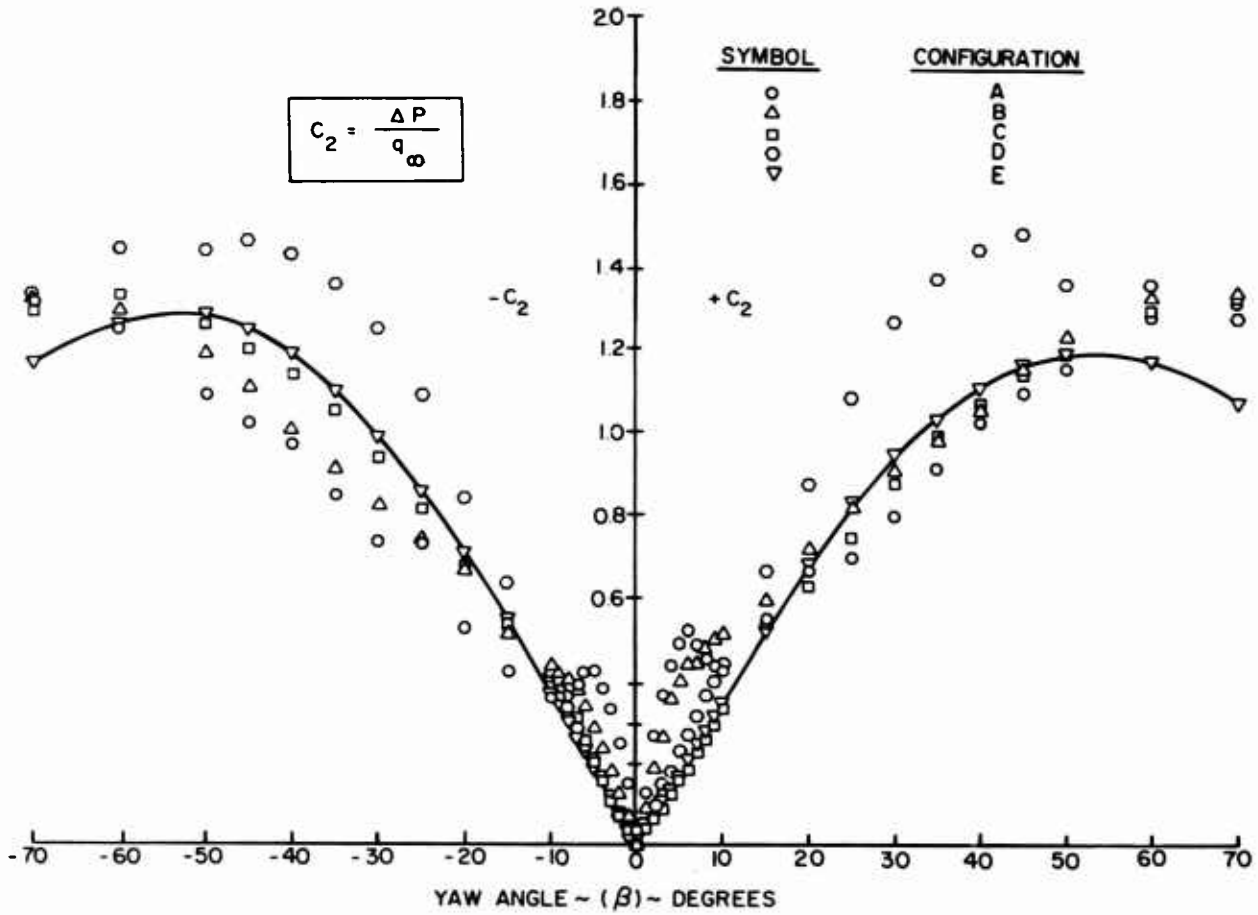

Figure 5c. Yaw Sensitivity - Sensitivity of Differential Pressure to Yaw (All Configurations).

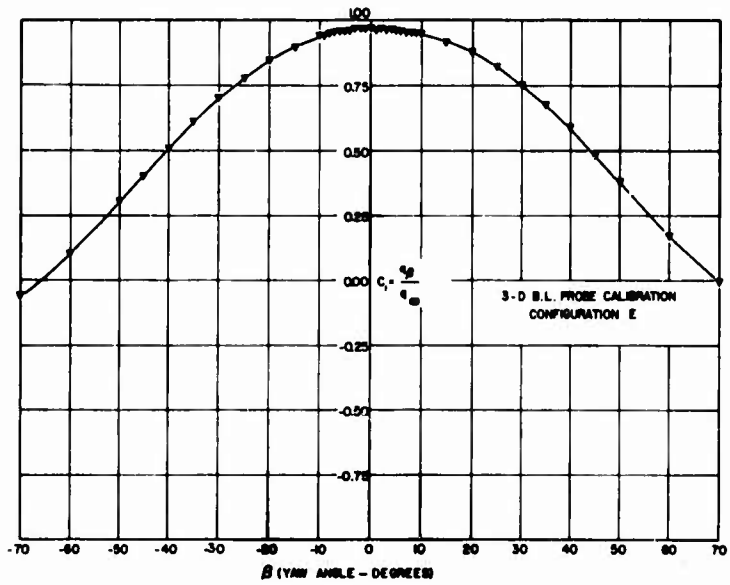

Figure 6a. Yaw Sensitivity - Sensitivity of Total Head to Yaw for Probe Configuration E.

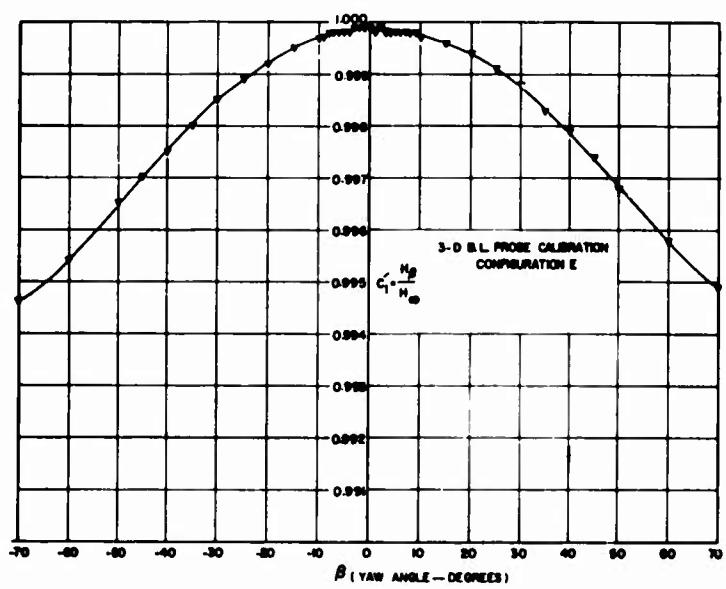

Figure 6b. Yaw Sensitivity - Sensitivity of Dynamic Pressure to Yaw for Probe Configuration E.

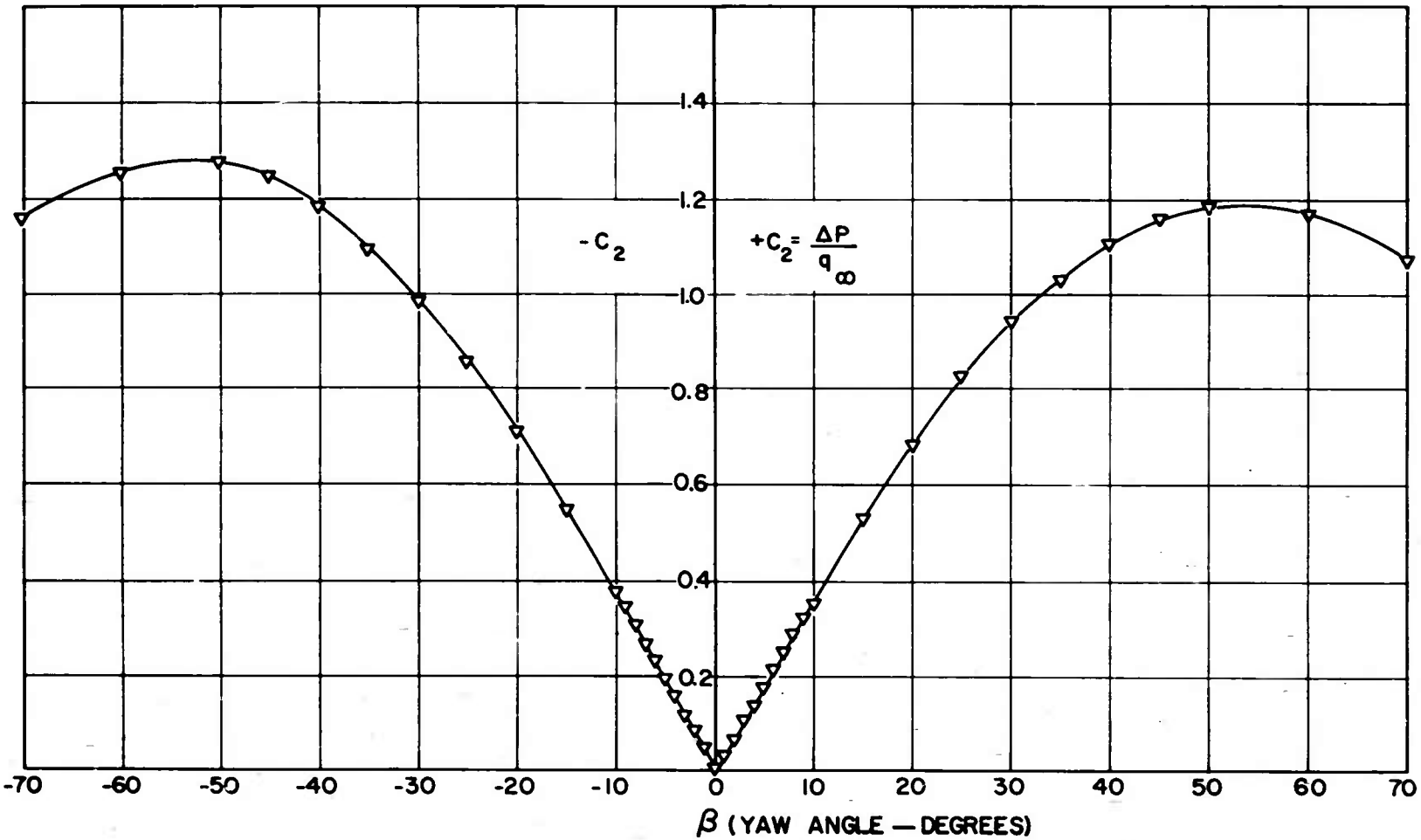

Figure 6c. Yaw Sensitivity - Sensitivity of Differential Pressure to Yaw for Probe Configuration E.

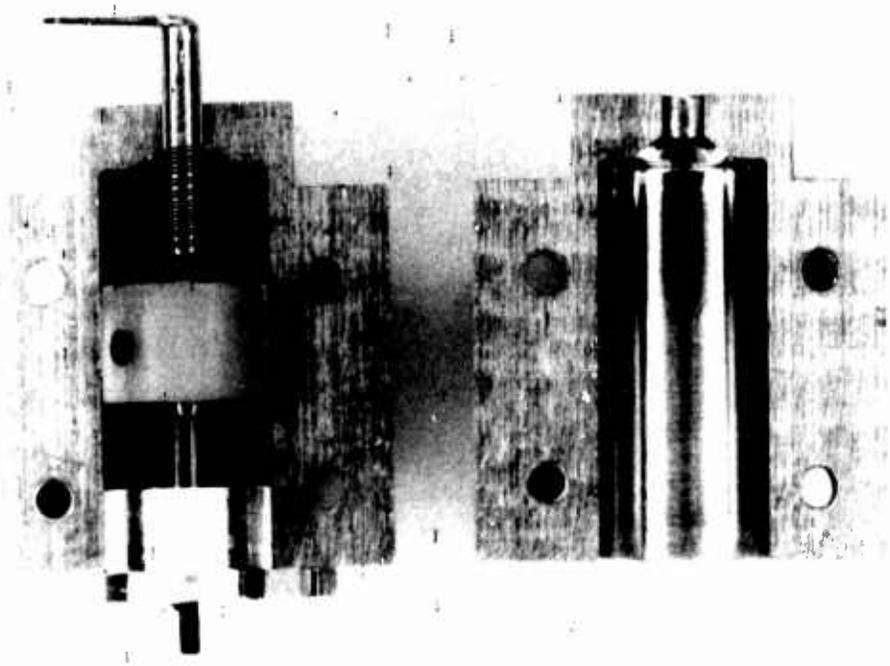

Figure 7. Exploded View of Manually Operated Boundary Layer Probe.

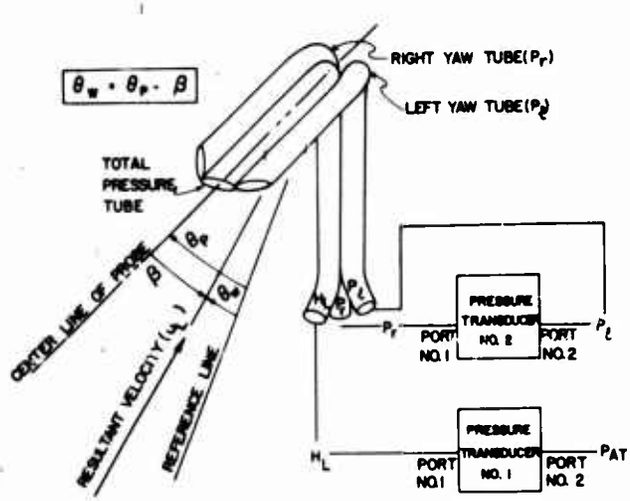

Figure 8. Schematic of Pressure Tubes and Pressure Transducers.

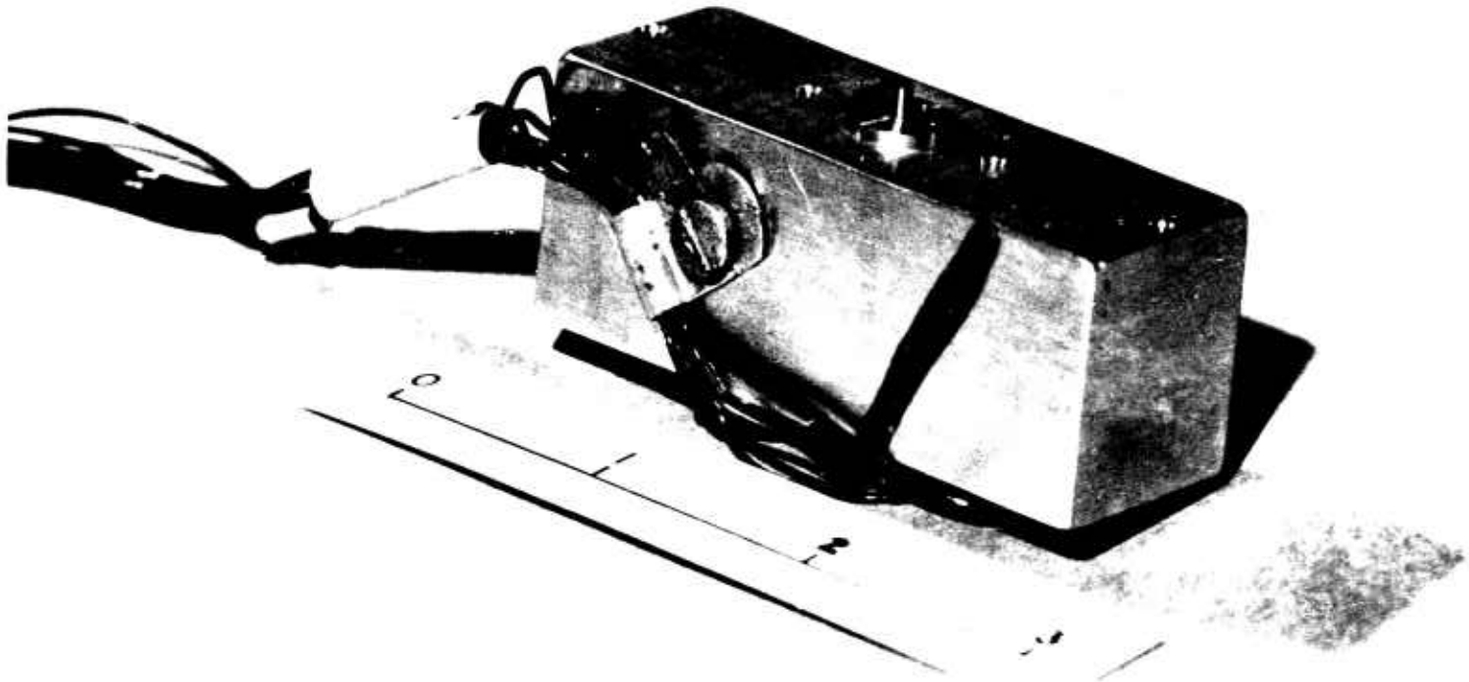

Figure 9. Oblique View of Initial Probe Unit.

Reproduced from best available copy.

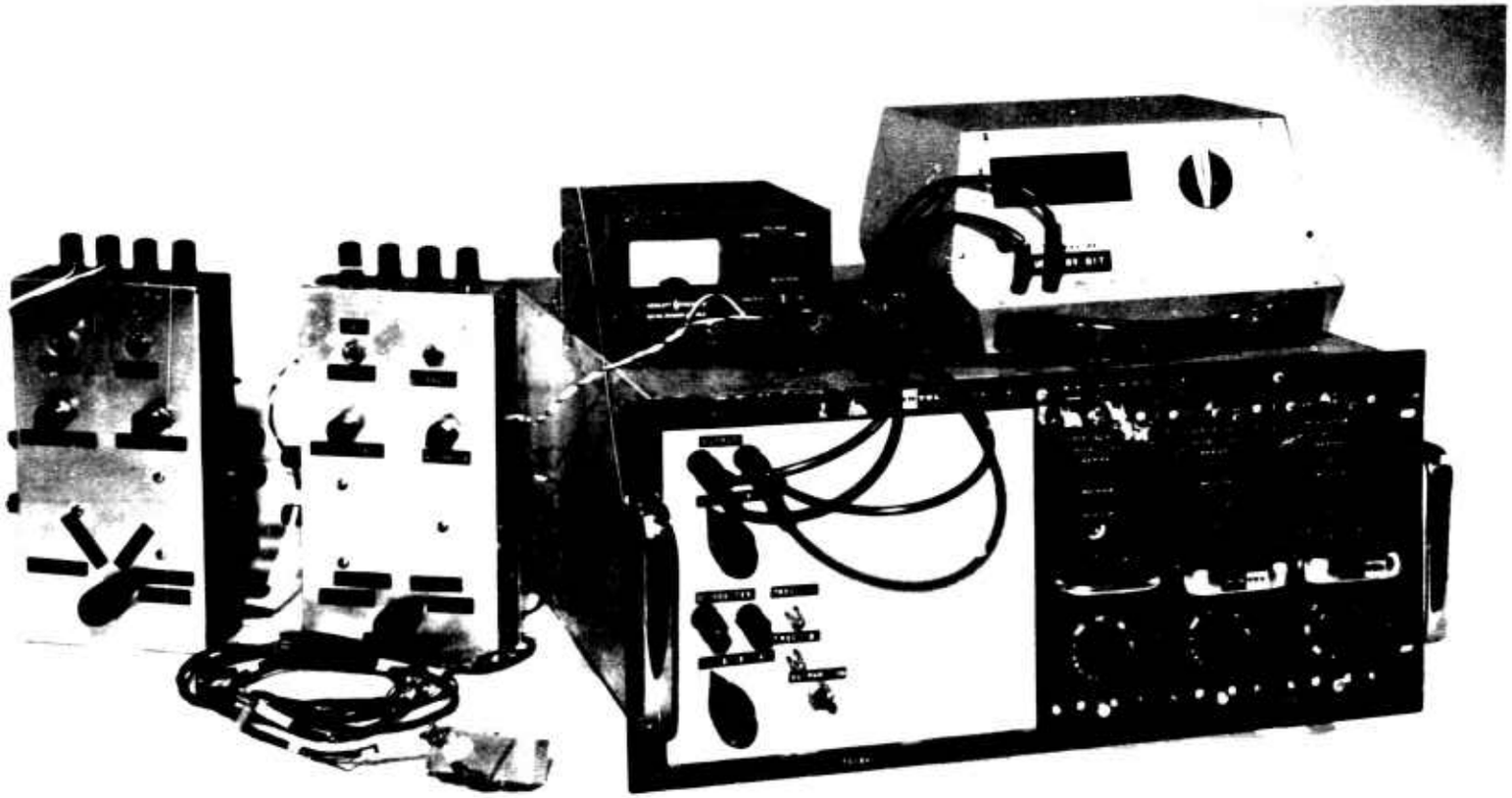

Figure 10. Photograph of Three-Dimensional Probe and Related Instrumentation.

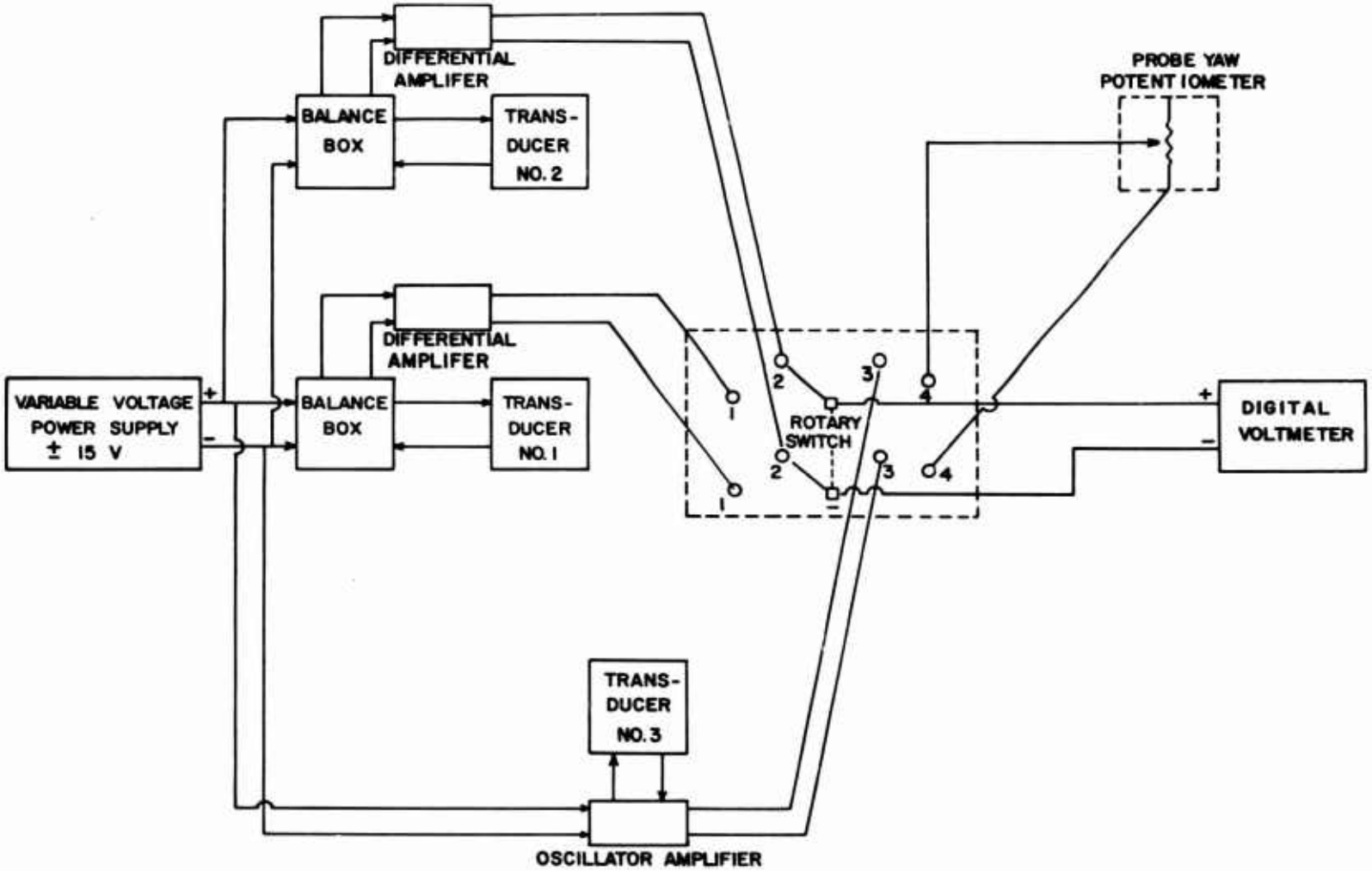

Figure 11. Schematic of Complete Instrumentation Electrical System.

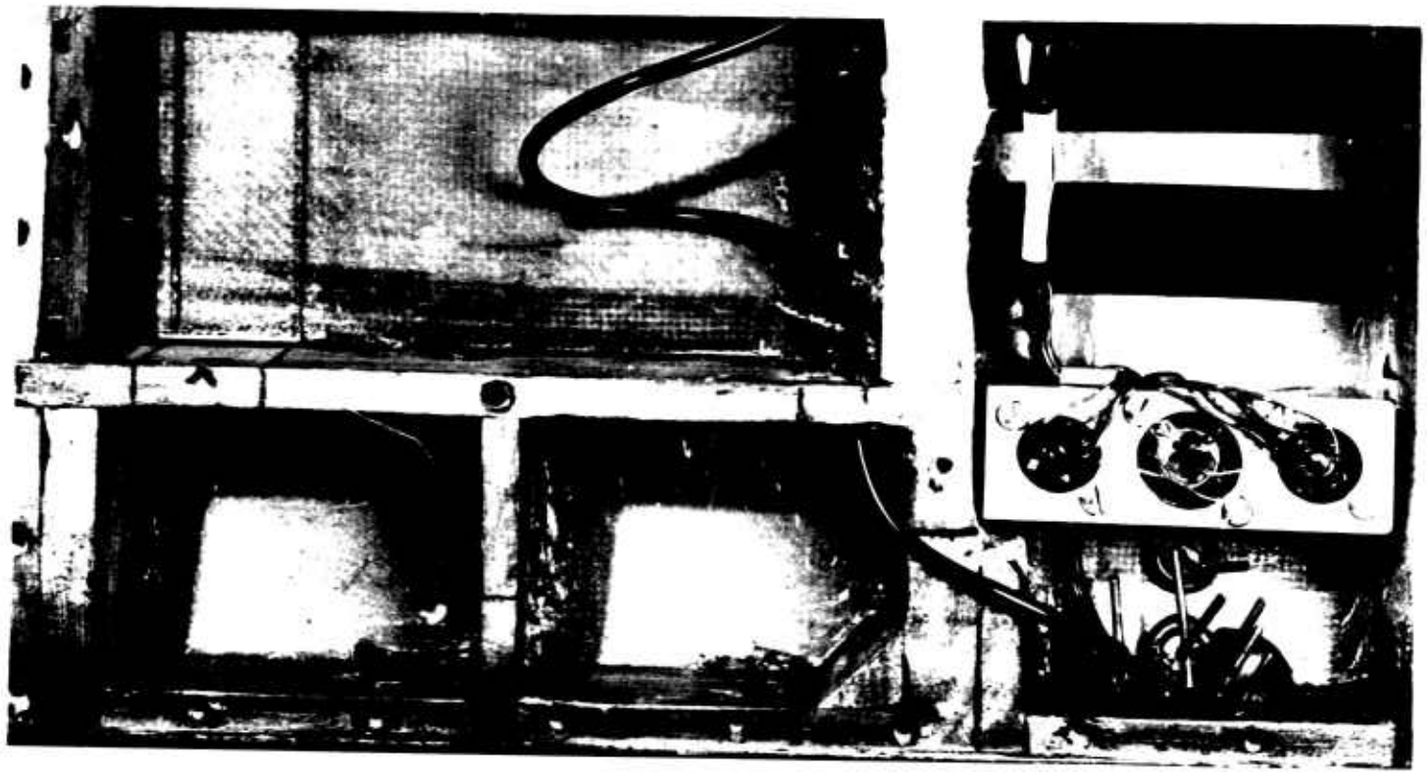

Figure 12. Installation of Boundary Layer Probe in Original Wing Model.

Reproduced from best available copy.

Figure 13. Yawed Wing Model Mounted in Subsonic Wind Tunnel.

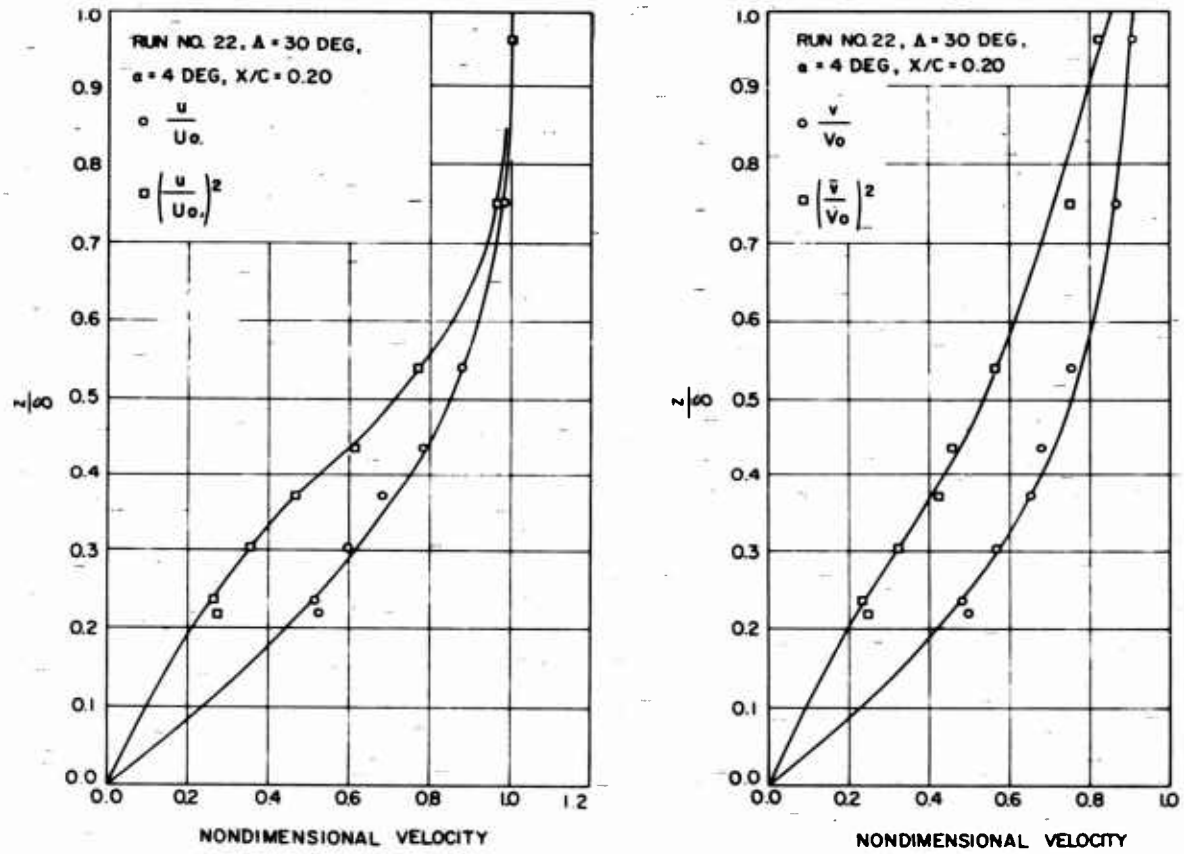

Figure 14a. Boundary-Layer Velocity Profiles Measured on a Yawed Wing, NACA 0012, R = 8.33 x 10^5, Laminar Profile.

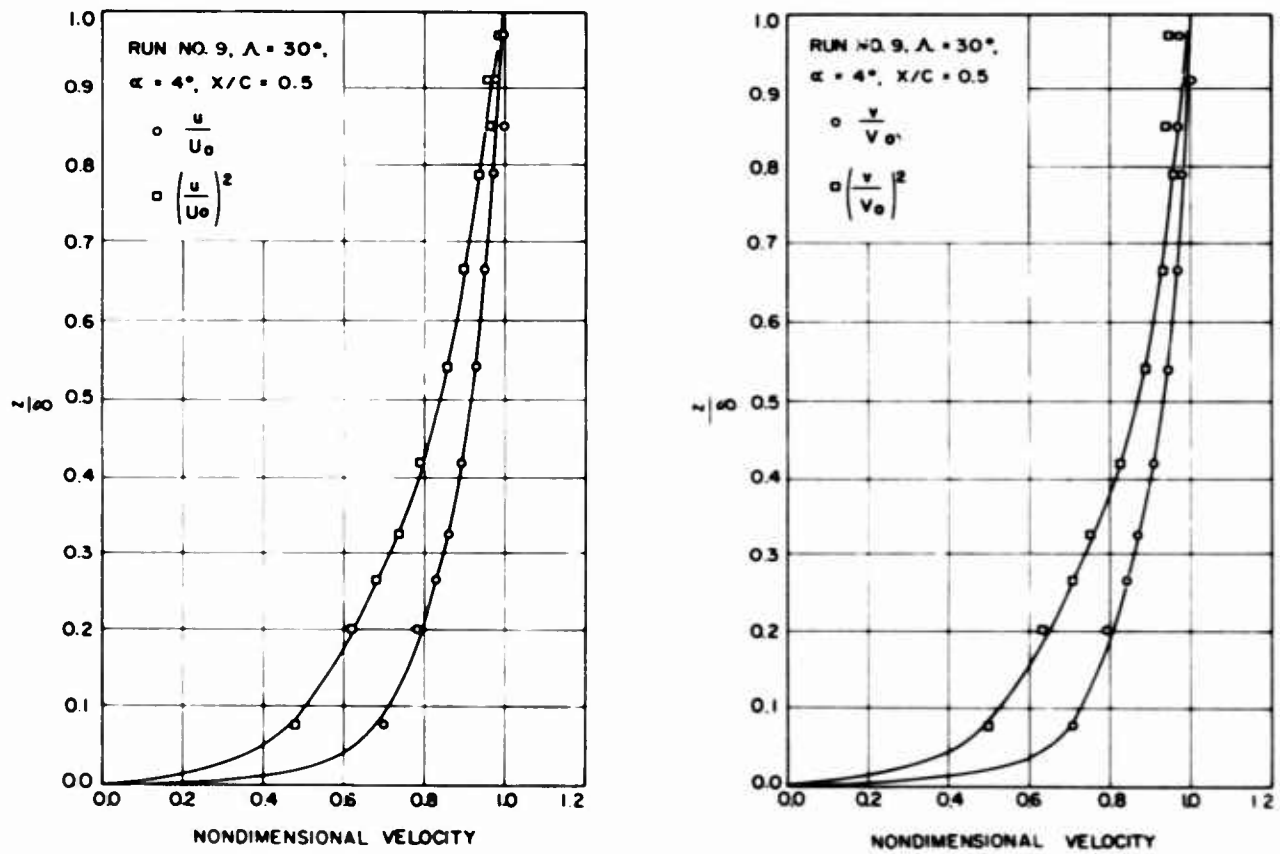

Figure 14b. Boundary-Layer Velocity Profiles Measured on a Yawed Wing, NACA 0012, R = 8.33 x 10^5, Turbulent Profile.

Figure 15. Exploded View of Remotely Operated Boundary Layer Probe.

Reproduced from best available copy.

Figure 16. Photograph of Remotely Operated Boundary Layer Probe.

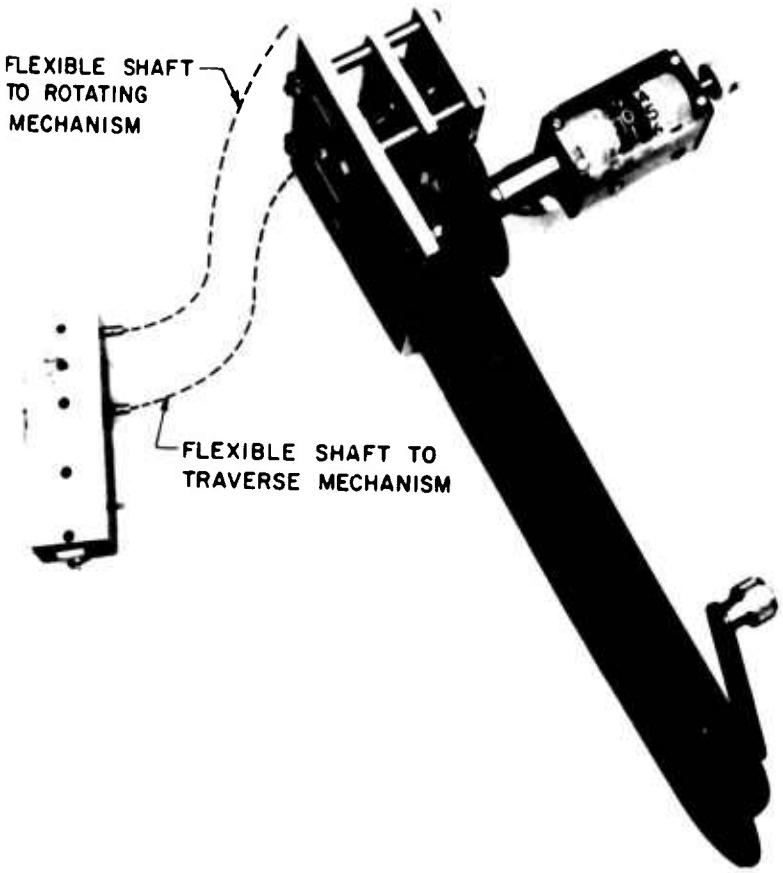

Figure 17. Photograph of Remotely Operated Boundary Layer Probe.

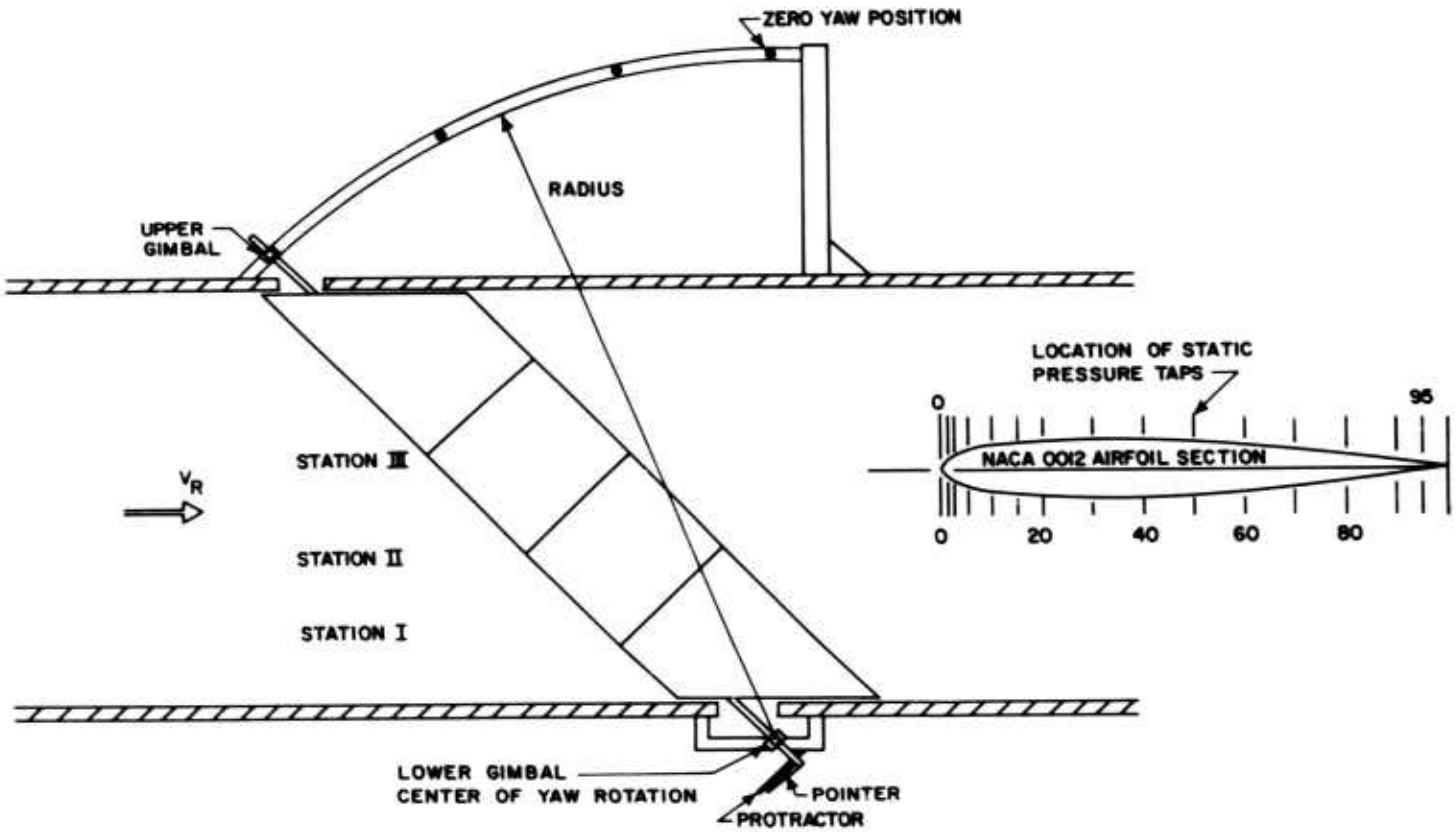

Figure 18. Schematic of Wing Model Mounted in Wind Tunnel.

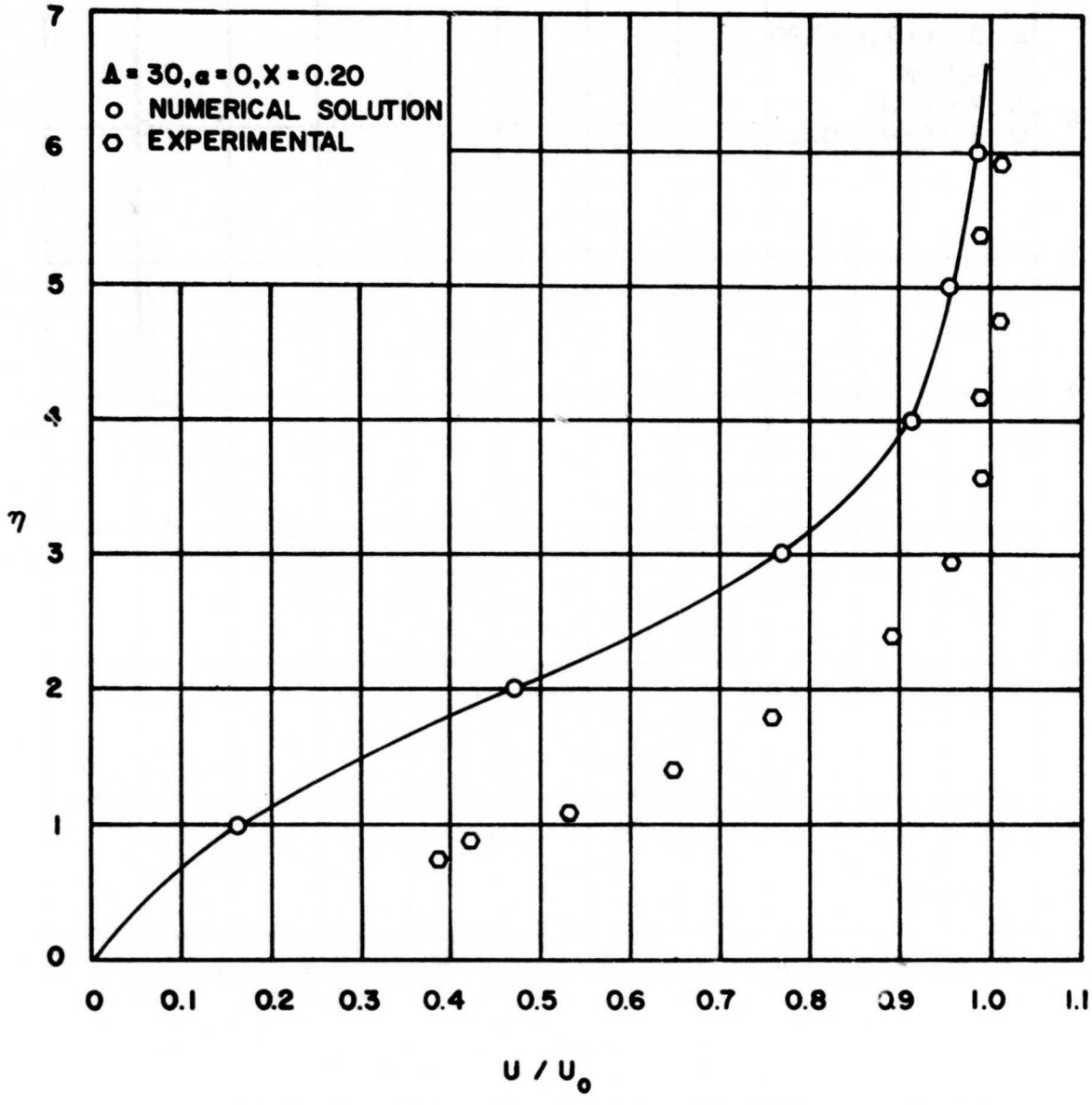

Figure 19. Chordwise Boundary-Layer Velocity Profile, $\Lambda = 30°$, $\alpha = 0°$, $x = 0.20$.

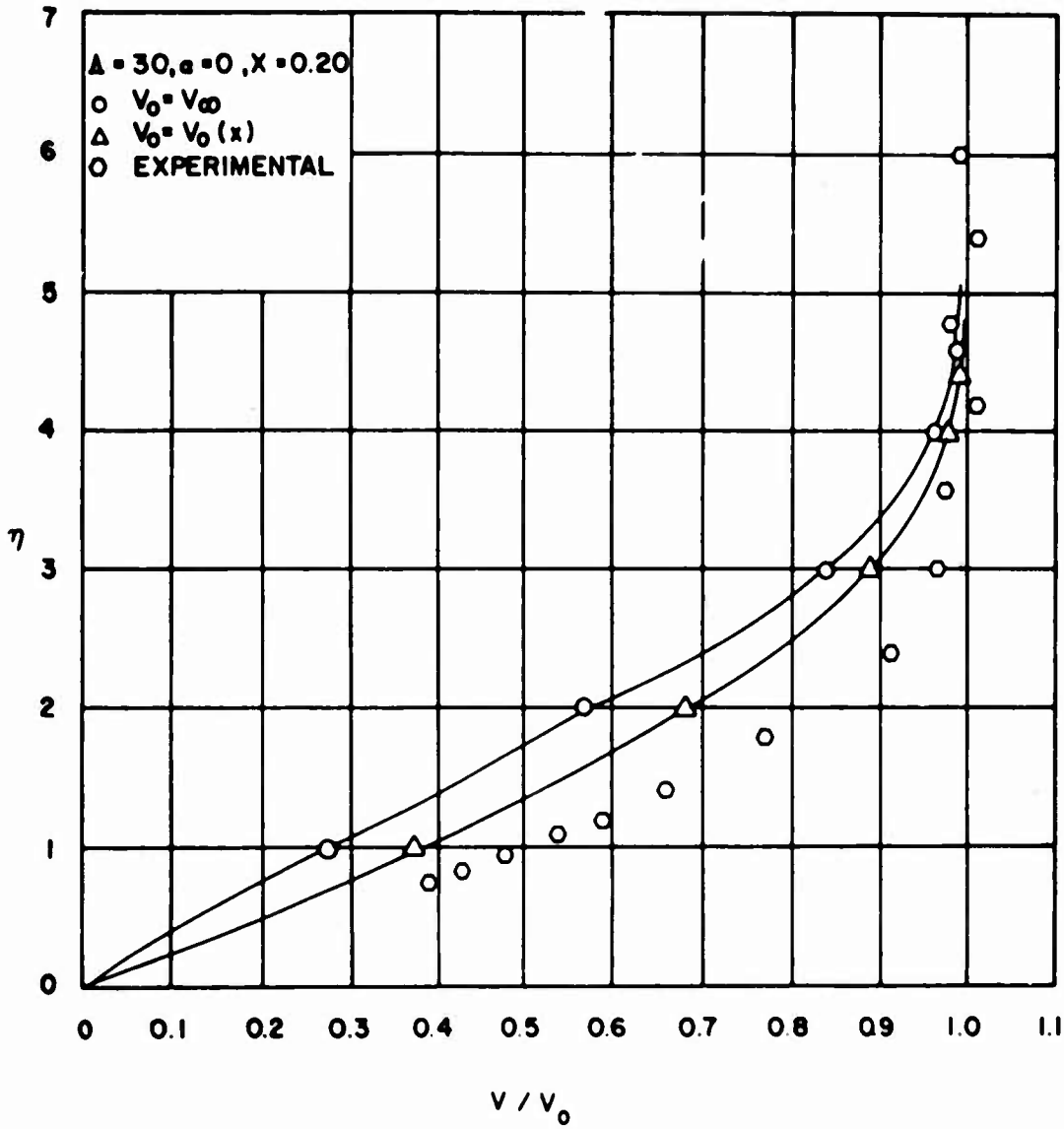

Figure 20. Spanwise Boundary-Layer Velocity Profile, $\Lambda = 30°$, $\alpha = 0°$, $x = 0.20$.

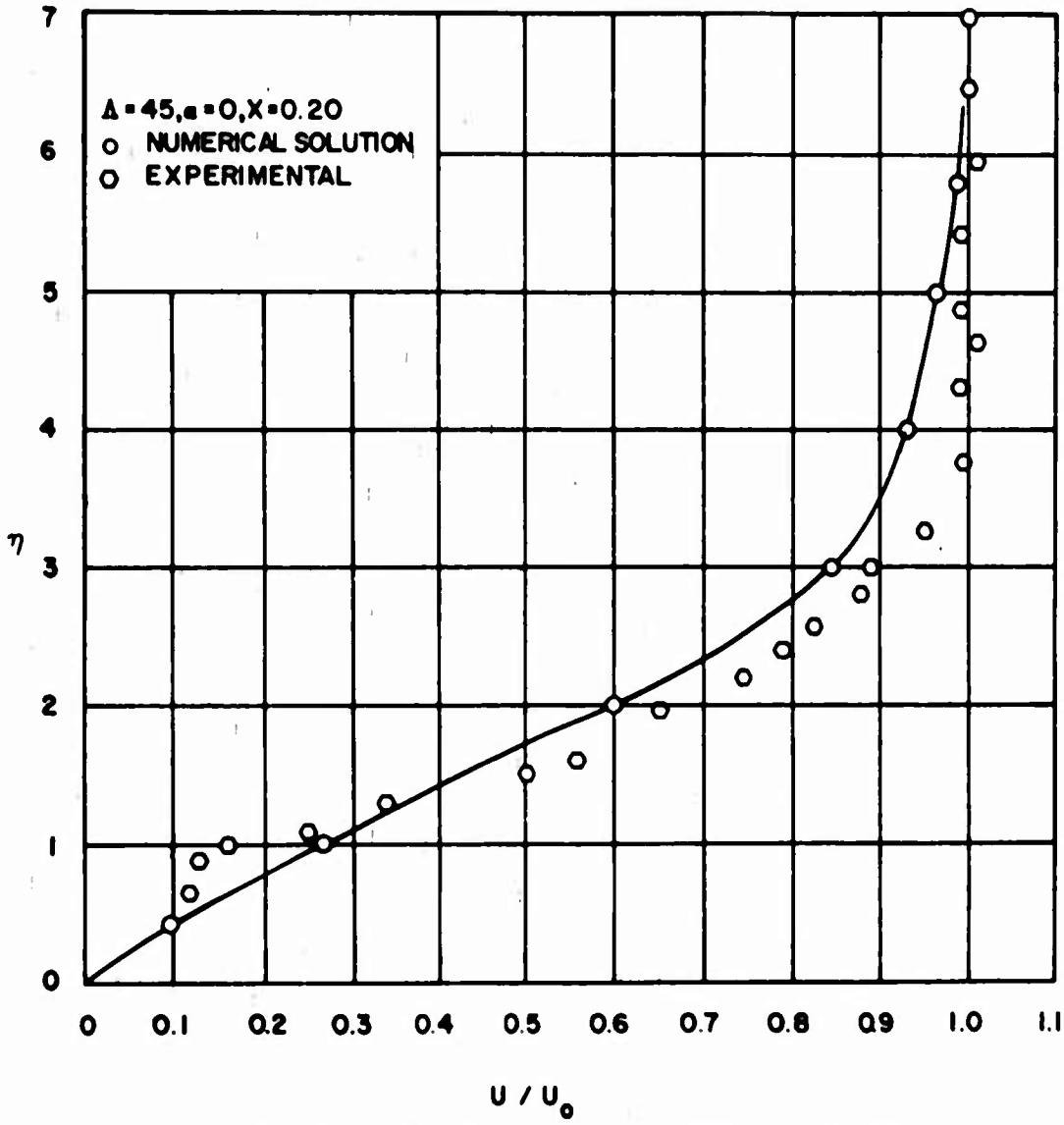

Figure 21. Chordwise Boundary-Layer Velocity Profile, $\Lambda = 45°$, $\alpha = 0°$, $x = 0.20$.

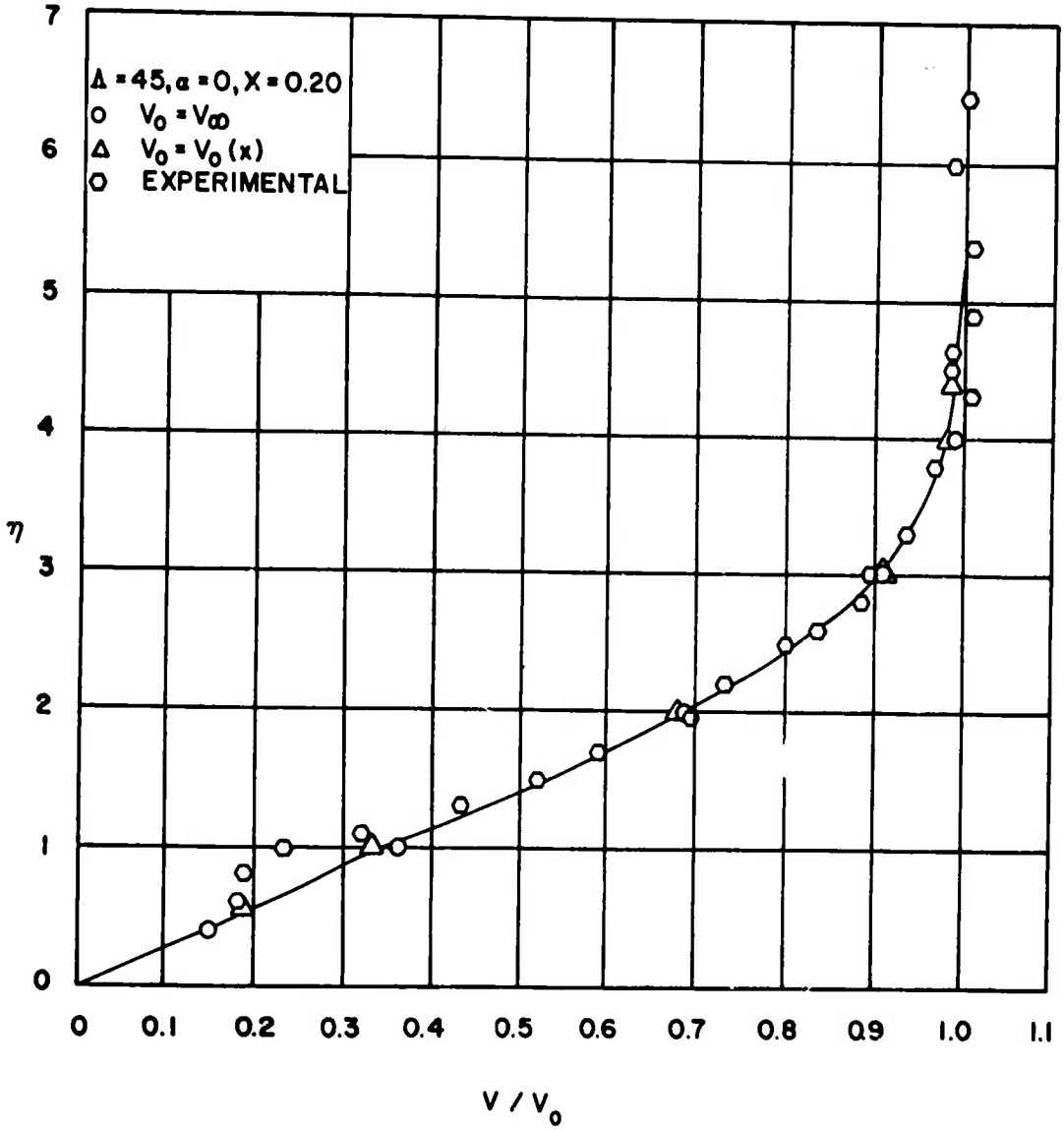

Figure 22. Spanwise Boundary-Layer Velocity Profile, $\Lambda = 45°$, $\alpha = 0°$, $x = 0.20$.

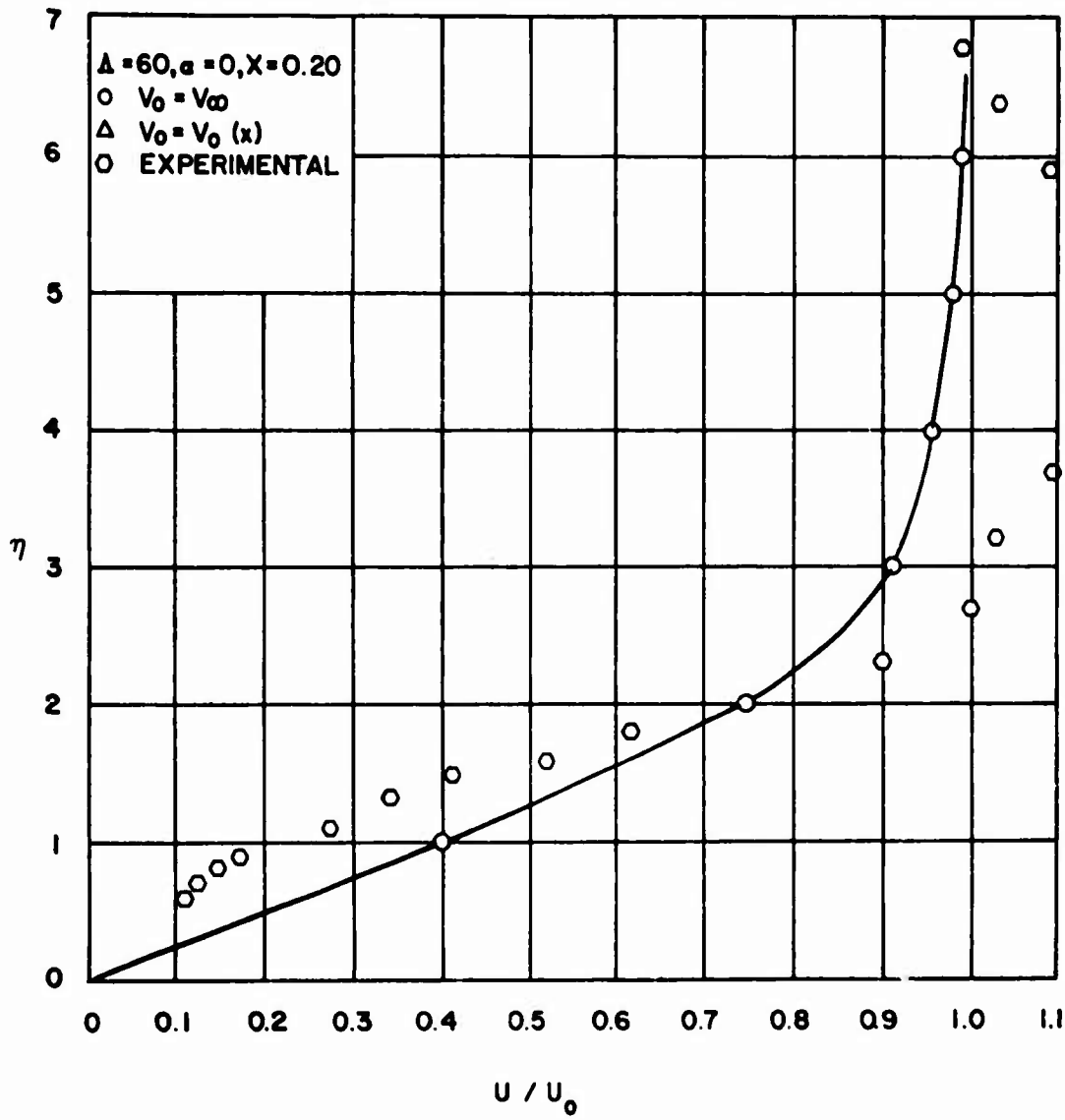

Figure 23. Chordwise Boundary-Layer Velocity Profile, $\Lambda = 60°$, $\alpha = 0°$, $x = 0.20$.

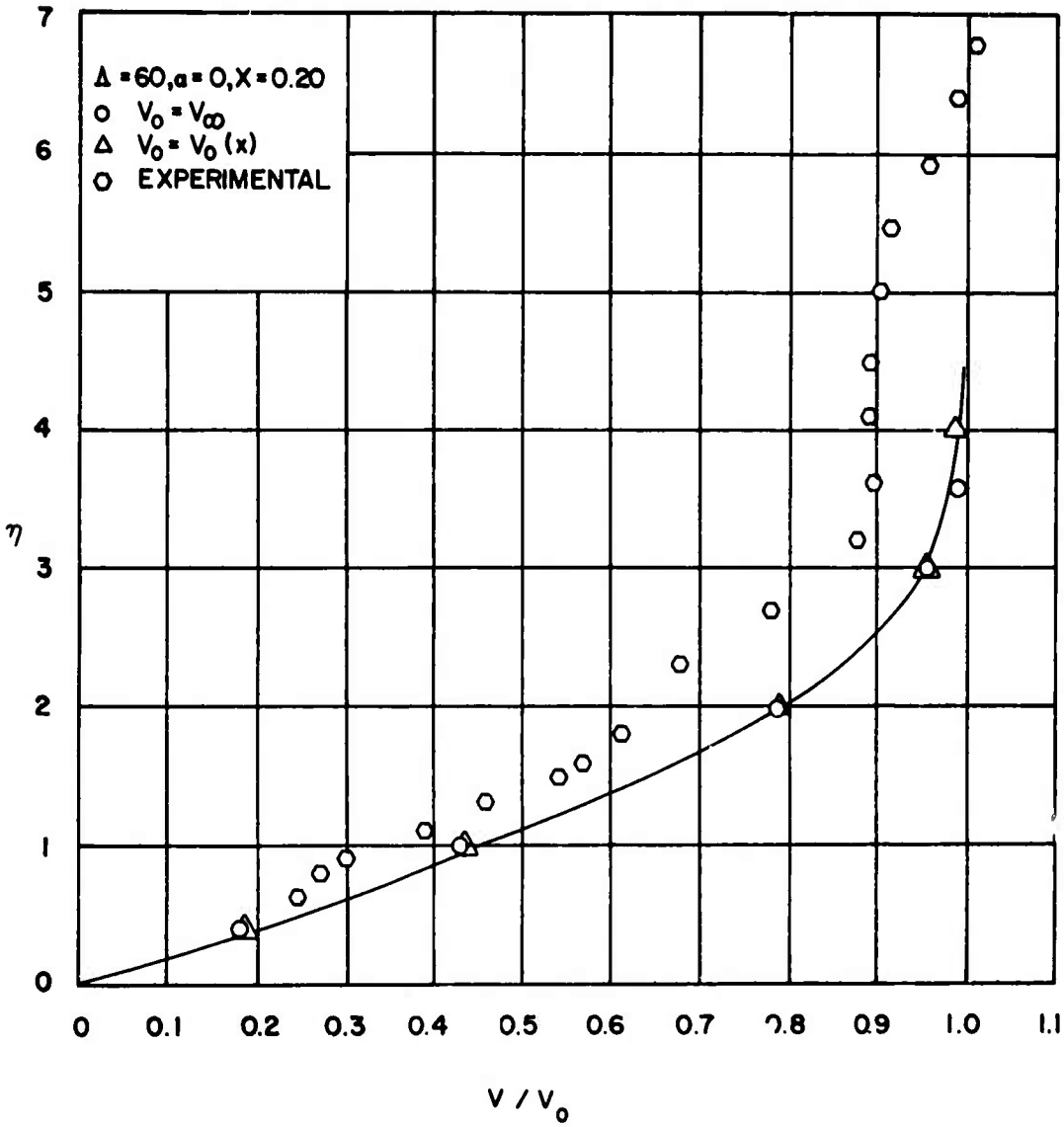

Figure 24. Spanwise Boundary-Layer Velocity Profile, $\Lambda = 60°$, $\alpha = 0°$, $x = 0.20$.

LITERATURE CITED

1. MacMillan, F. A., VISCOUS EFFECTS ON FLATTENED PITOT TUBES, Astia Rept. 570836, AD 135487, July 1957.

2. Bradshaw, P., and Goodman, D. G., THE EFFECTS OF TURBULENCE ON STATIC PRESSURE TUBES, ARC R and M No. 3527, 1966.

3. Ower, E., and Pankhurst, R. C., THE MEASUREMENTS OF AIR FLOW, Pergamon Press, 4th Edition, 1966.

4. MacMillan, F. A., EXPERIMENTS ON PITOT-TUBES IN SHEAR FLOW, ARC R and M No. 3028, 1957.

5. Smith, Michael R., THREE-DIMENSIONAL BOUNDARY LAYER FLOW OVER YAWED WINGS, Ph.D. Dissertation, Department of Aerophysics and Aerospace Engineering, Mississippi State University, State College, Mississippi, August 1970.